Ph.D. Thesis

Development of absolute quantification method by nuclear magnetic resonance using internal reference substance with SI traceability

（内部標準を利用する NMR 分光法による絶対定量法の開発）

Graduate School of Bioresources
Mie University

Tsuyoshi KATO

March 2019

Ph.D. Thesis

Development of absolute quantification method by nuclear magnetic resonance using internal reference substance with SI traceability

（内部標準を利用する NMR 分光法による絶対定量法の開発）

Graduate School of Bioresources
Mie University

Tsuyoshi KATO

March 2019

Contents

Abbreviations

1,4-BTMSB-d_4	1,4-bis(trimethylsilyl)benzene-d_4
2D-TLC	two-dimensional thin-layer chromatography
2-LOPA	2-lyso-oleoylphosphatidic acid
2-LPA	2-lysophosphatidic acid
2-LPS	2-lysophosphatidylserine
AQARI	accurate quantitative NMR with internal standard material
CFP	ciguatera fish poisoning
CRM	certified reference material
CTX(s)	ciguatoxin(s)
CTX1B	ciguatoxin-1B
CTX3C	ciguatoxin-3C
CTX4A	ciguatoxin-4A
DSS-d_6	3-(Trimethylsilyl)-1-propanesulfonic acid-d_6 sodium salt (4,4-dimethyl-4-silapentane-1-sulfonic acid-d_6 sodium salt)
DHSM	dihydrosphingomyelin
DOPC	dioleoylphosphatidylcholine
DOPS	dioleoylphosphatidylserine
DSPG	distearoylphosphatidylglycerol
DSPA	distearoylphosphatidic acid
DSPE	distearoylphosphatidylethanolamine
DTX1	dinophysistoxin-1
EDTA	ethylenediaminetetraacetic acid
ELSD	evaporative light scattering detectors
epideoxyCTX1B	52-*epi*-54-deoxyciguatoxin-1B

^{1}H NMR	proton nuclear magnetic resonance
51hydroxyCTX3C	51-hydroxyciguatoxin-3C
IS(s)	internal standard(s)
LPC	lysophosphatidylcholine
LPE	lysophosphatidylethanolamine
LPI	lysophosphatidylinositol
NMR	nuclear magnetic resonance
OA	okadaic acid
PA	phosphatidic acid
PC	phosphatidylcholine
PE	phosphatidylethanolamine
PG	phosphatidylglycerol
PI	phosphatidylinositol
^{31}P NMR	phosphorus nuclear magnetic resonance
POPE	palmitoyloleoylphosphatidylethanolamine
POPG	palmitoyloleoylphosphatidylglycerol
PS	phosphatidylserine
PSER	phosphoserine
qNMR	quantitative nuclear magnetic resonance
SI	international system of units
SM	sphingomyelin
SOPC	stearoyloleoylphosphatidylcholine
T_1	relaxation time
TRM	traceable reference material

General Introduction

Nuclear magnetic resonance (NMR) spectroscopy is a method for observing the spin state of nuclei. This spectroscopy is possible to identify the molecular structure of the target compound using the difference in the magnetic environment at the functional group or the nuclear level, furthermore, the number of its nuclei can be directly and accurately quantified. Figure 1 shows the proton nuclear magnetic resonance (^{1}H NMR) spectrum of ethanol. In the spectrum, signals of hydrogen nuclei constituting the methyl (CH_3), the methylene (CH_2) and the hydroxyl (OH) groups are observed, respectively, and their signal intensity ratios are 3: 2: 1. As described above, NMR can be used not only to obtain information about the type of the functional groups, but also the number of nuclei, so it has been widely used as a quantitative analysis technique in the field of structural analysis. In organic synthesis, the reaction recovery rate can be known from the number of specific functional groups before and after the reaction. This is an advantage of NMR spectroscopy that can simultaneously perform qualitative and quantitative analysis. The quantitative test by NMR is in particular called quantitative NMR[1-3] in distinction from qualitative application.

Among the methods for quantitative NMR, pulse length-based concentration measurements (PULCON)[4] which separately measures standard solution and test solution. A coaxial double tube method, which simultaneously measures standard and test materials existing in the inner and outer tube of special test tube. Furthermore, there are also electronic referencing to access *in vivo* concentrations (ERETIC)[5] and quantification by artificial signal (QUANTAS)[6], which standardize the intensity of the electric signal artificially generated on the spectrum. The above methods are called external standard methods and have advantages that the sample is secured from the contamination with standard materials. On the other hand, the method with the sample is dissolved in the solution containing the standard material is called the

IS (internal standard) method, which the sample cannot be secured from the contamination with standard materials, however it is the most accurate method among quantitative NMR[7].

In 2008, a specific quantitative nuclear magnetic resonance (qNMR) method using the IS was developed in Japan, and this was particularly called accurate quantitative NMR with internal standard material (AQARI)[8-10]. The uncertainty in the quantitative value determined by AQARI is less than 1%[11,12]. In addition, certified reference materials (CRM) dedicated to qNMR were developed at the same time, and 3-(Trimethylsilyl)-1-propanesulfonic acid-d_6 sodium salt (DSS-d_6) and 1,4-bis(trimethylsilyl)benzene-d_4 (1,4-BTMSB-d_4) showing single-line signals around 0 ppm could be used as ISs for AQARI. Such CRM makes it possible to give traceability to the International System of Units (SI) for the quantity of many substances[13]. AQARI or its analogous method[14] can be utilized as a remarkable method to determine the purity of low molecular organic compounds. The purity determination by employing AQARI will contribute to the improvement of quality and reliability of analytical results obtained by the general-purpose instrument analysis such as chromatography[15].

In this study, the author investigated, upper limit of molecular weight of the target substances and lower limit of the sample concentration of test solution for a quantitative test using AQARI. Marine biotoxins with cyclic polyether structure are challenging substances as qNMR targets because of their high molecular weight and limited availability. In the first study, AQARI was chosen for the purity determination method of the diarrhetic shellfish poisoning causative toxins, okadaic acid (OA) and its analogous substance dinophysistoxin-1 (DTX1). Here, the author established a new method that enables to use AQARI while avoiding contamination by the involatile ISs. Due to the very limited amount of the toxins usable, it was difficult to obtain sufficient signal intensity, because the concentration of the sample was low, so the processing method was optimized in order to obtain the closest quantitative value to true value. In the second study, the author accomplished to determine the accurate quantity of ciguatoxins (CTXs) in order to prepare the accurately quantified materials as reference standard

for a wide-variety of instrumental analysis such as HPLC, GC/MS, and LC/MS. These were even larger molecules and available in seriously limited amounts. The institute of the author belongs, Japan Food Research Laboratories, started service which these precious quantified samples are distributed to the researcher in world-wide as reliable standard material. In the third study, the author validated the effectiveness of phosphorus nuclear magnetic resonance (^{31}P NMR) as a quantitative technique using nuclides other than hydrogen nuclei. In NMR spectroscopy, the sensitive nuclei are ^{1}H, ^{19}F and ^{31}P. Although ^{31}P is next to ^{19}F in sensitivity, it is included in many natural and synthesized compounds with bioactivity, so it is contained in phospholipids. In the individual quantification of phospholipid classes, two-dimensional thin-layer chromatography (2D-TLC) method or HPLC with evaporative light scattering detectors (ELSD) have been mainly used, however the author payed attention to ^{31}P NMR, which could be separate and quantify each phospholipid class due to difference in polar group. In the previous applications on qNMR, different protocols were reported, and performance as quantitative methods of ^{31}P NMR have not been sufficiently verified. For this reason, the author optimized the measurement conditions of ^{31}P NMR in which SI traceable IS containing phosphorus, phosphoserine was introduced.

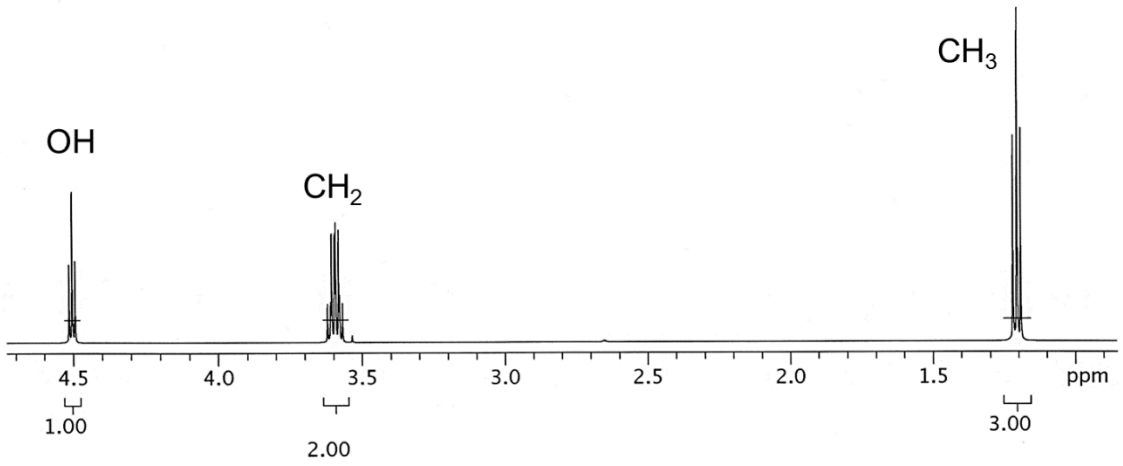

Fig. 1 ^{1}H NMR spectrum of ethanol (CH_3-CH_2-OH).

Chapter 1

Absolute Quantification of Lipophilic Shellfish Toxins Using Quantitative Nuclear Magnetic Resonance with Removable Internal Reference Substance with SI Traceability

1.1 Introduction

A lipophilic shellfish toxin, OA, is a large and complex marine toxin[16, 17] produced by the dinoflagellates e.g. *Dinophysis fortii*[18] and *Prorocentrum lima*[19]. That has been detected in filter-feeding bivalve shellfish, such as oysters, mussels, scallops and clams, which prey on the dinoflagellates having toxin. The conventional method for monitoring toxic shellfish is the mouse bioassay[20]; however, there has been a shift to using instrumental analysis techniques, such as LC/MS[21-24] to identify and quantify the target shellfish toxin among various toxins. Consequently, the demand for authentic shellfish toxin standards has risen; yet, the sources of such shellfish toxin standards are limited to the toxic shellfish and cultured dinoflagellates. In addition, laborious steps are required for extraction and purification; therefore, the purified shellfish toxins are extremely precious.

As a worldwide toxin reference supplier, Canada employed qNMR earlier than others[25, 26]. qNMR is one of the best quantitative methods to calibrate precious materials, including shellfish toxins[27]. It has the following two main advantages: (1) samples can be recovered because qNMR is a non-destructive method, and (2) the NMR signal intensity is theoretically directly proportional to the molar concentration of a sample so a single measurement is enough for accurate quantification without the use of a calibration curve. However, the analysis of large molecules (>800 Da), such as OA and DTX1, is challenging for qNMR because their complex structural features—numerous proton nuclei and diverse conformations—cause partial spectral overlap. Moreover, the use of CRMs of involatile materials is disadvantageous because they can

cause contamination.

In the present study, OA and DTX1 were quantified based on the AQARI technique, pyridine and the residual proton in methanol-d_4 were used as the ISs. They are removable substances which had calibrated beforehand using a maleic acid CRM served. A rigorous determination of the purity of OA and DTX1, and its ability to serve as a reliable reference standard were accomplished through selecting the adequate proton signals for quantification and examining the concentration dependence of the signal intensity.

1.2 Experimental

1.2.1 Reagents and chemicals

OA ($C_{44}H_{68}O_{13}$, ca. 60 mg) and DTX1 ($C_{45}H_{70}O_{13}$, ca. 10 mg) were extracted from poisonous shellfish and supplied by co-researchers Yasumoto *et al*. These lipophilic shellfish toxins exhibited almost only one peak in the total ion chromatogram of LC/MS. OA and DTX1 were dried *in vacuo* in a desiccator containing diphosphorus pentoxide for at least 20 days. NMR test tubes with a 5 mm outer diameter were purchased from Kusano Science Co. (Tokyo, Japan). Methanol-d_4 (99.96% deuterium content) was obtained from Merck KGaA (Darmstadt, Germany), pyridine (guaranteed reagent, 99.8%) from Sigma-Aldrich Co. LLC. (St. Louis, MO, USA), and the maleic acid certified reference material (purity 99.7%, expanded uncertainty was 0.9%, k = 2) from FUJIFILM Wako Pure Chemical Corporation (Osaka, Japan).

1.2.2 Apparatus

The experimental setup was composed of a semi-micro balance (AG285, Mettler-Toledo, Greifensee, Switzerland), an ultra-micro balance (MSE2.7S, Sartorius AG, Göttingen, Germany), and an NMR spectrometer equipped with a Varian 5-mm indirect probe (Varian NMR System 500, Varian Technologies, Palo Alto, CA, USA).

1.2.3 Preparation of test solutions containing pyridine as an IS

Twenty microliters of pyridine was diluted using 4 mL of methanol-d_4. OA (20.1 mg) and the maleic acid CRM (2.26 mg) were accurately weighed. Each was then dissolved in 1 mL of the above solution to afford the methanol-d_4 solutions of OA containing pyridine as the IS and the methanol-d_4 solution of pyridine containing the maleic acid CRM, respectively.

1.2.4 Preparation of test solutions containing residual proton of methanol-d_4 as an IS

The maleic acid CRM (1.46–2.64 mg) and ampules of methanol-d_4 (0.669 g (average), ca. 0.8 mL) were accurately weighed and mixed to afford the test solutions of maleic acid CRM (N = 5) containing the residual proton of methanol-d_4 as the IS. OA (8.99 mg) and DTX1 (4.27 mg) were also accurately weighed and dissolved by the contents in the weighed ampule of methanol-d_4 (0.674 and 0.667 g, ca. 0.8 mL) to prepare the OA (11 mg/mL) and DTX1 (5.1 mg/mL) solutions containing the residual proton of methanol-d_4 as the IS.

1.2.5 ^{1}H NMR measurements

For ^{1}H NMR experiments, the relaxation delay was six times or above the longest relaxation time (T_1) of pyridine signals to recover over 99% of z-magnetization[9]; T_1 was previously determined by an inversion-recovery test. The following settings were used for AQARI experiments: irradiation frequency, 499.868 MHz; acquisition time, 4 s; relaxation delay, 60 s; probe temperature, 7 or 25 °C; spectral width, 40.332 ppm; FID data points, 161,288; number of scans, 8–2,560; spinning, off; pre-scans, two times; ^{13}C decoupling, MPF8; pulse angle, 90°; pulse width, 10.4 μs.

1.2.6 Data processing

Data was processed with VnmrJ software ver. 2.3 supplied by the manufacturer (Varian Inc.). Fourier transformation was performed on 262,144 data points. All proton chemical shifts

were referenced to the residual proton signal in methanol-d_4 (CD_2HOD) at 3.300 ppm. A phase of all spectra was collected manually while observing spectral line shape. The baseline of spectra was adjusted horizontality, and each signal area ratio was calculated by software functions. An integration range was individually optimized based on the line width of signals and the space between the signals. The spectra were integrated using the spectral bucketing technique with 0.002-ppm-sized buckets. The area ratio of each signal was calculated by adding all buckets larger than buckets arising from the baseline (noise level).

1.2.7 Determination of pyridine (IS) concentration

The quantity of pyridine in the solution was determined using a ^{1}H NMR spectrum of the maleic acid–pyridine solution by the following equation (1):

$$Value_A = \frac{I_A}{I_{IS}} \times \frac{N_{IS}}{N_A} \times \frac{M_A}{M_{IS}} \times W_{IS} \times P_{IS} \qquad (1)$$

$$P_A = \frac{I_A}{I_{IS}} \times \frac{N_{IS}}{N_A} \times \frac{M_A}{M_{IS}} \times \frac{W_{IS}}{W_A} \times P_{IS} \qquad (2)$$

where $Value_A$ is the quantity of a target compound (g); I_A is the area ratio of each individual signal resulting from the target compound; I_{IS} is the area ratio of the IS; N_{IS} is the number of protons of the IS; N_A is the number of protons of the target compound; M_A is the mole weight of the target compound; M_{IS} is the mole weight of the IS; W_{IS} is the weight (g) of the IS; P_{IS} is the purity (w/w%) of the IS; P_A is the purity (w/w%) of the target compound; and W_A is the weight (g) of the target compound. The quantity was calculated using total area of pyridine signals (P1-P3 are shown in Fig.2) as 5 protons to be 0.00591 g.

1.2.8 Determination of the quantity of CD_2HOD in methanol-d_4

The quantity of CD_2HOD was calculated using the ^1H NMR spectra of the solution of maleic acid CRM dissolved in methanol-d_4. Employing maleic acid as the IS, the CD_2HOD purity was determined to be 0.117% (0.1% RSD; $N = 5$) using the equation (2) provided above.

1.2.9 Evaluation of the dispersion in the quantitative value affected by the phase corrections

The ^1H NMR spectrum of DTX1 was measured by 1, 8, and 16,824 transient accumulations. The signal area ratios were obtained by 20 repetitions of integration and calibration; the repetitions were also used for repeatability calculations.

1.2.10 Concentration dependence of the OA spectra

^1H NMR spectra of OA were obtained for 0.01, 0.09, 0.5, 1, 4, and 11 mg/mL of OA. Accurately weighed OA samples (ca. 1, 4, and 9 mg) and methanol-d_4 (0.61–0.68 g, ca. 0.8-0.9 mL) were mixed to afford the test solutions. The OA test solutions containing 0.01, 0.09, and 0.5 mg/mL of OA were prepared by diluting the solution containing 1 mg/mL of OA with methanol-d_4.

1.2.11 Evaluation of trueness

OA quantification was performed in triplicate (from sample solution preparation to qNMR measurement) for all OA concentrations (0.01, 0.09, 0.5, 1, and 4 mg/mL) except 11 mg/mL (single measurement). The trueness (%) was determined from division of the individual quantity by the purity of OA.

1.3 Results and Discussion

1.3.1 Measurement of OA and DTX1 spectra

^{1}H NMR spectra of OA and DTX1 are shown in Fig. 2. Assignment of each signal was based on the reference[28]. Both spectra were very similar because the structural difference between OA and DTX1 is limited to the presence or absence of the methyl group at position 35. The proton signals belonging to the saturated hydrocarbon groups were inappropriate for quantification because of the degree of overlap. In contrast, signals A–K, arising from the protons on unsaturated or oxygenated carbons, were moderate- or well-separated, and hence, those were used for quantity calculations. The signal F, H and J were composed more than two protons. Also signal C composed two insufficiently separated signals and thus treated together. However, signal D, near the water signal, was excluded from quantification. The measurement temperature was set so that the water signal position was adjusted to the center of signals C and E.

1.3.2 Determination of OA purity

A spectrum having sufficient signal intensity (S/N>1,000) was obtained by eight transients using 20 mg/mL of OA. The area between the lower and upper ^{13}C satellite signals has been reported to be a reliable integration range to obtain accurate area ratios[29]; however, this area was only applicable to signals E, FG and P1–P3. Signals A–K and P1–P3 were integrated by a spectral bucketing and the binning technique with 0.002-ppm-sized buckets. The signal area ratios were calculated as a sum of bins, which were larger in size than that of the baseline region (Range A, Fig. 3). The average quantified value based on the integration of Range A using signals A–K and total of P1–P3 as the IS was 97.6% with RSD 0.89% (Table 1) using the equation (2) provided above. In addition, the signal area ratios for E and FG were also integrated from the area between the ^{13}C satellite signals (Range B). The quantified values of signals E and FG employing Range B were 97.3% (0.20% RSD) and 97.4% (0.02% RSD),

respectively. Those are very well consistent with that by Range A. Hence, the purity of OA was established to be 97.4% with traceability to the SI units.

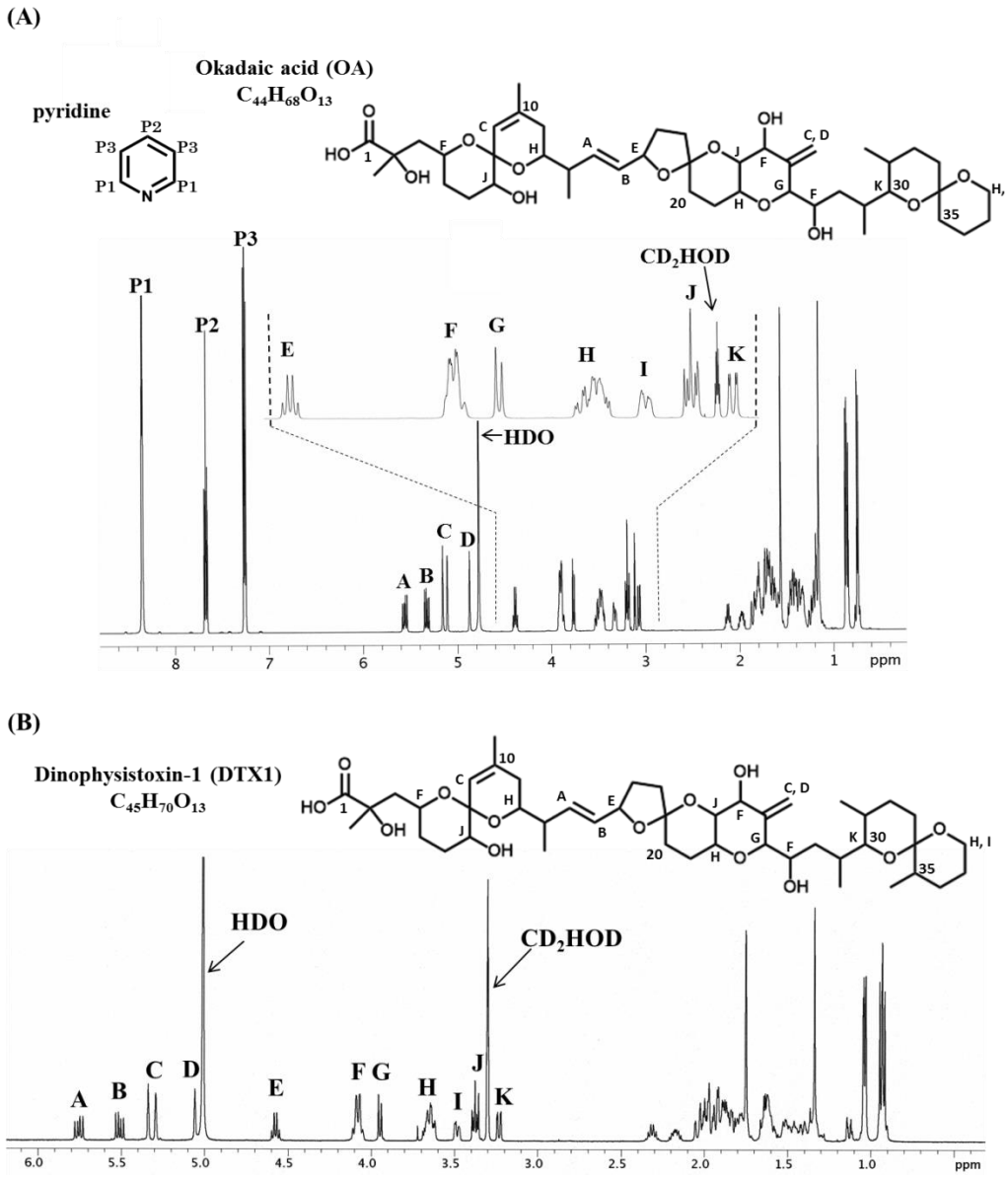

Fig. 2 ^{1}H NMR spectra of OA and DTX1.

(A) OA (20.1 mg weighed) in methanol-d_4 (1 mL) with 5 µL of pyridine as IS; probe temp, 25 °C; 8 transients; spinning, off; ^{13}C decoupling, MPF8.

(B) DTX1 (4.27 mg weighed) in methanol-d_4 (0.67 g weighed; ca. 0.85 mL) as IS (CD_2HOD); probe temp, 7 °C; 8 transients; spinning, off; ^{13}C decoupling, MPF8.

The signal C is composed of two signals.

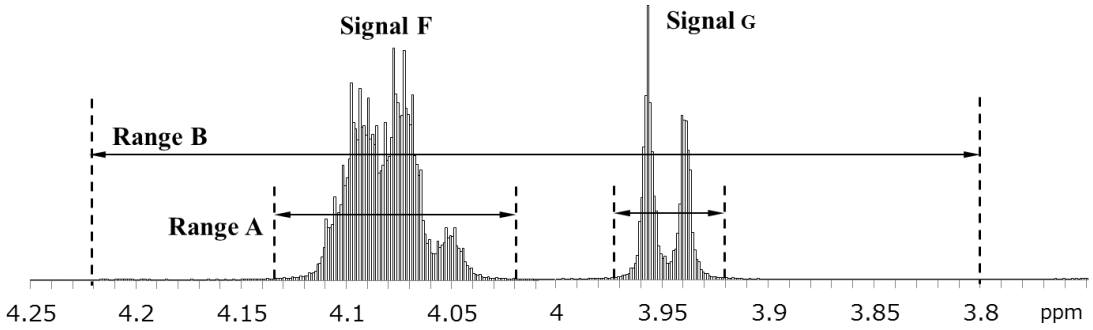

Fig. 3 Integration ranges applied to DTX1 signals (typical example).

Range A, integration ranges were optimized to the individual signals; Range B, integration range was based on the lower and upper ^{13}C satellite signals. The signal areas were integrated with a bucketing technique with 0.002-ppm-sized buckets.

1.3.3 Applicability of residual proton in methanol-d_4 as an IS

The residual proton in methanol-d_4, CD_2HOD, was also suited to be the IS. Although the T_1 of the residual proton (10 s) was a little longer than that of pyridine (P1, 7.0 s, P2, 7.5 s, and P3, 6.9 s) in methanol-d_4, the concentration of residual proton was consistently stable (within an error of 0.1% RSD) for much of 10 h. However, the signal of CD_2HOD was proximally close to signals J and K, so the measurement temperature was optimized to avoid overlap. The area ratio of CD_2HOD was successfully determined to be 99.6% when compared to the theoretical value using solely CD_2HOD without OA at 7 °C. Table 2 shows the quantified results of OA (11 mg/mL) and DTX1 (5.1 mg/mL) using CD_2HOD as the IS. Those values of OA (Table 2) were consistent with those from when pyridine served as the IS (Range A, Table 1). DTX1 was quantified by the same method. The amount of CD_2HOD in the ampules of methanol-d_4 was found to be consistent within the same lot of reagents (0.1% RSD, N = 5). In order to use the pyridine IS solution, it had to be prepared before every commencing use. Thus, the use of the residual proton CD_2HOD improved working efficiency by reducing sample preparation steps and eliminating an external calibration. It succeeded in obtaining the traceability to the SI units for absolute quantity measurement of shellfish toxin standards.

Table 1 Calculated purity of OA (20 mg) using pyridine as the IS.

Signals	Number of Protons	Integration		Purity	
		Range	Width (ppm)	Value (%)	RSD (%)
P1 as IS	2		0.300	-	-
P2 as IS	1		0.260	-	-
P3 as IS	2		0.280	-	-
A	1		0.232	96.4	0.2
B	1		0.200	98.7	0.1
C	2		0.230	98.5	0.1
E	1	Range A	0.206	97.3	0.2
F	3		0.182	97.0	0.1
G	1		0.154	99.0	0.3
H	3		0.208	97.0	0.1
I	1		0.106	97.8	0.2
J	2		0.132	97.4	0.1
K	1		0.140	96.9	0.3
P1 as IS	2		0.399	-	-
P2 as IS	1		0.326	-	-
P3 as IS	2	Range B	0.409	-	-
E	1		0.372	97.3	0.2
FG	4		0.399	97.4	0.1

Table 2 Calculated purity of OA (9 mg) and DTX1 (4 mg) using CD_2HOD in methanol-d_4 as the IS.

Signals	Number of Protons	Integration		Purity	
		Range	Width (ppm)	Value (%)	RSD (%)
CD_2HOD as IS	1		0.054	-	-
E	1	Range A	0.206	97.8	0.1
FG	4		0.336	97.6	0.1
CD_2HOD as IS	1	Range A	0.061	-	-
FG_{DTX1}	4		0.318	97.9	0.1

1.3.4 Accuracy related to the phase correction process

The accuracy associated with the phase correction process was examined using the spectrum of DTX1 (Fig. 4). The obtained spectra were subjected twenty times to the phase correction, integration and calibration process. With an increasing number of transients, the signal-to-noise ratios tended to improve, and the repeatability of each signal also decreased; however, the magnitude of improvement was significantly different for each signal. Signals A–D had relatively larger phase fluctuations than others because of interference from the intense water signal. The repeatability of signals F, H, and J, which involved multiple protons, was lower than those involving single protons (signals A, B, D, E, G, I, and K), and were superior for quantification because they were less affected by phase fluctuation.

1.3.5 Effect of OA concentration on the signal shape

The effect of OA concentration on the signal shapes was investigated in cases of spectra using 0.01, 0.09, 0.5, 1, 4, and 11 mg/mL of OA (Fig. 5). The signals A, E, and H, significantly broadened in line shape with reducing OA concentration. Particularly, signal A essentially disappeared at 0.01 mg/mL of OA. The carboxyl group at position 1 of OA has been reported to form a cavity-like structure with the hydroxyl group at position 24 by intramolecular hydrogen bonding[17,30]. Therefore, the signal was most likely affected under low concentrations by the significant conformational disorder at the highly flexible part of the OA skeleton around the corresponding protons. Signal A showed broader line width and lower intensity than signal B, which is on the opposite side of the double bond. Thus, the signal A was an unreliable for quantification. For OA less than 0.4 mg/mL, signal E was also not reliable presumably based on the above mentioned conformational disorder.

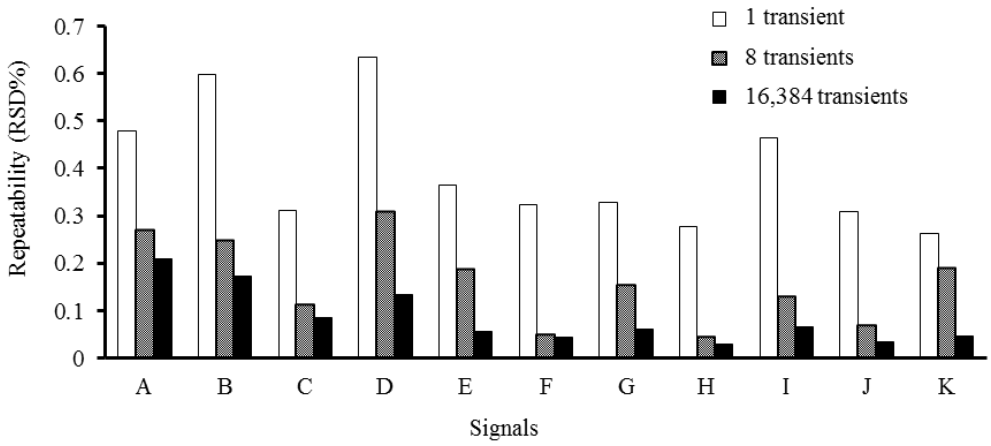

Fig. 4 Repeatability of phase correction for signals A–K on NMR spectrum of DTX1.

The process of phase correction was repeatedly applied 20 times to the spectra of DTX1 obtained from the measurement by 1, 8, and 16,384 transients (signal-to-noise ratio of the smallest signal was 100, 300, and 2,500 respectively).

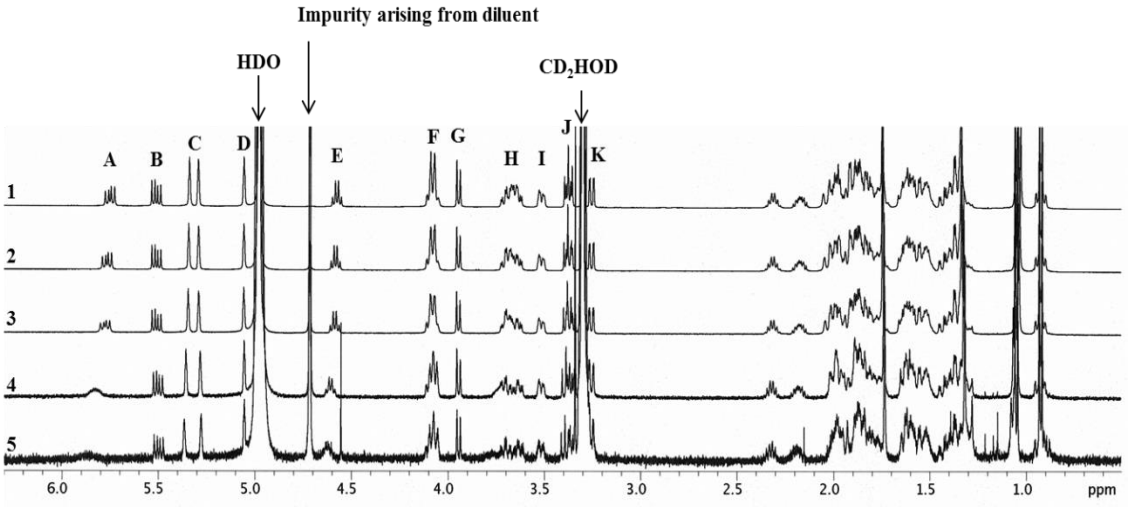

Fig. 5 Concentration dependent change of ^{1}H signals in OA spectra.

1, OA 4 mg/mL; 2, OA 1 mg/mL; 3, OA 0.5 mg/mL; 4, OA 0.09 mg/mL; 5, OA 0.01 mg/mL

1.3.6 Evaluation of trueness

Figure 6 shows the relationship between the OA concentration (mg/mL) and trueness (%) of quantitative values. The trueness calculated from signal A and E tended to deviate from the theoretical value as the concentration decreased. The trueness values calculated from 11 or 4 mg/mL of OA showed nearly 100% of trueness using Range A as well as Range B area integration methods; however, values deviated from the theoretical value for Range B area

integration for low concentrations (>0.1 mg) in comparison to that of Range A. This was an effect of Range B being more sensitive to the increased noise level. The area at the part of baseline tended to be increased with rising noise level, with exception of the signal A and E which broadened under less OA concentration (Fig. 6). Therefore, the present study revealed that Range A, where the integration range was optimized for the individual signals, should be employed unless a spectrum obtained from more than 4 mg/mL of OA. Considering the subjectivity caused by phase correction, signal F or FG was the best choice for OA quantification. Although accurate quantification of OA was accomplished by qNMR, the accuracy was admittedly dependent on the amount of OA available. For qNMR using the aforementioned signals, the trueness was 100.1% (0.39% RSD) for 4 mg/mL, 100.1% (1.3% RSD) for 0.09 mg/mL, and 112.1% (1.5% RSD) for 0.01 mg/mL. Thus the author judged that the authenticity of the purity of OA and DTX1 should be obtained from the data using more than 4 mg of toxins.

1.4 Conclusions

OA (20.1 mg and 8.99 mg) and DTX1 (4.27 mg) were weighed, used for preparing of test solutions, and measured utilizing an NMR instrument with a proton resonance frequency of 499.87 MHz. OA and DTX1 were accurately quantified by qNMR, using the well-separated proton signals attached to the oxygenated carbons, to afford reference toxin standards having an authentic purity (97.4% and 97.9% respectively). The residual proton CD_2HOD in methanol-d_4 was beneficially used as an IS, which was able to be removed afterward, and to avoid contaminating the precious shellfish toxins. Using the residual proton significantly improved working efficiency due to the simplification of the sample preparation and calibration. The applicability of OA quantification by AQARI was established using the calibrated OA standard. Our findings showed that the integration range should be optimized for individual signals unless a sufficient amount of OA affords a spectrum having adequate intensities—more than 0.1

mg/mL of OA is highly recommended to use for AQARI to suppress the deviation (less than 5%) from the true value.

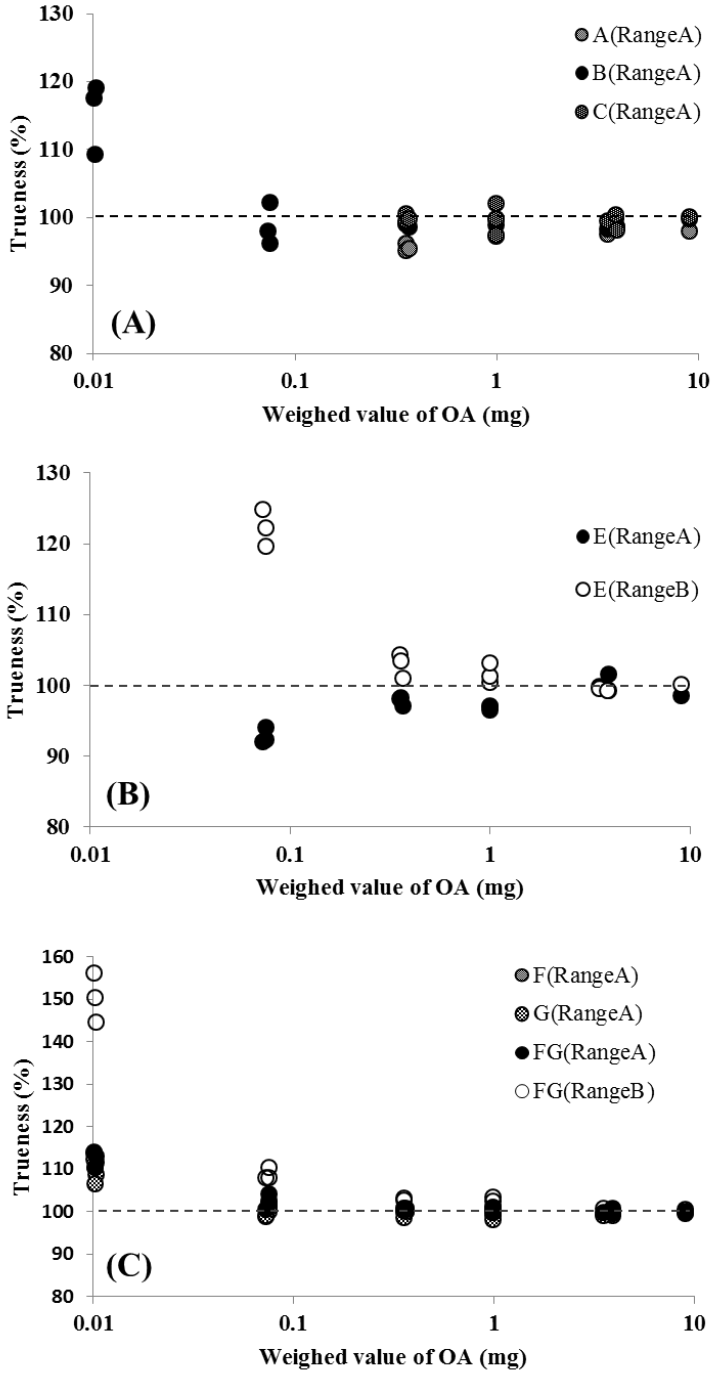

Fig. 6 The correlation between the OA concentration and its trueness calculated from signals A, B, C, E, F, G, and FG.

Each data point represents three individual experiments except for 11 mg/mL (single measurement). (A), signals A, B, and C (Range A); (B), signal E (Range A and B); (C), signals F, G, FG (Range A), and signal FG (Range B).

Chapter 2

Quantification of Representative Ciguatoxins in the Pacific using Quantitative Nuclear Magnetic Resonance Spectroscopy

2.1 Introduction

Ciguatera fish poisoning (CFP) refers to a peculiar form of neurologic poisoning resulting from the ingestion of fish inhabiting warm water regions. Though the mortality rate is low, the morbidity rate for CFP is the highest among the poisoning of natural etiology, with an estimated number of around 50,000 patients annually[31]. In the Pacific, the causative toxins, named ciguatoxin (CTX), are produced by microalgae, *Gambierdiscus* spp., and accumulate in various species of fish *via* the food chain[32]. The toxicity of individual fish is unpredictable and markedly fluctuates, as the population of the causative alga and feeding history of fish can greatly vary[33]. To protect human health and avoid serious economic loss due to the implication of commercially important species, proper measures to detect toxins are highly desired. Mouse bioassays[34] have been the routine practice to detect CTXs since the early days but need to be substituted by other methods of higher sensitivity and specificity, not to mention the call to limit animal use for routine assays. Previously, the author proposed using an LC/MS method as an alternative and successfully revealed the details of regional and species variations of toxin profiles in fish and causative algae[35]. The method is highly sensitive and produces accurate data, but the author has to clear three hurdles to promote its wide use. First, the author has to quantify extremely low concentrations of the toxins. The consensus on the regulation level is 0.01 ppb for ciguatoxin-1B (CTX1B) or its equivalent in flesh[36]. Even higher is the second hurdle to prepare pure toxins to be used as standards. The major toxin, CTX1B, needed four tons of toxic fish collected over ten years to obtain 0.35 mg. Much effort had to be continued, therefore, to prepare toxins of less abundance. The final problem to be solved was how to quantify such

minute samples. The toxins have no chromophore. Complete drying for weighing is defied because recovery from the vessel surface becomes difficult. Therefore, the author chose a qNMR method for quantitation. The foreseeable problems in NMR were; small amount of samples, multiple and often overlapping proton signals, the large ladder-shape structure comprising stereo-flexible medium size rings (seven, eight, and nine membered), and the large signals of water that remain in the samples. The routine practice of using CRM as an IS was disfavored to avoid the contamination of the target toxins with the nonvolatile CRMs. Instead, the author used CRM to quantify the residual protons in pyridine-d_5 and subsequently used the calibrated pyridine-d_5 as the secondary inner standard to quantify the CTXs. CTXs present in fish in the Pacific consist of two groups differing in their skeletal structures, CTX1B type, and ciguatoxin-3C (CTX3C) type. Hence, the selection of suitable protons in each type is required for quantification. The author carried out the NMR measurements, meticulously choosing the parameters. The quantity of each CTX was calculated by employing the signal area ratio accurately integrated between the CTXs and calibrated pyridine-d_5 proton signals. Thus, the author achieved, for the first time, the quantification of five toxins important in monitoring fish toxicity in the Pacific (Fig. 7): CTX1B, 52-*epi*-54-deoxyciguatoxin-1B (epideoxyCTX1B), CTX3C, 51-hydroxyciguatoxin-3C (51hydroxyCTX3C), and ciguatoxin-4A (CTX4A). The calibrated toxins will serve as an invaluable tool to identify and quantify the toxins in fish that have remained elusive in the past. A great contribution is expected to toxicology, epidemiology, environmental studies, and commercial fisheries.

2.2 Experimental

2.2.1 Materials

CTX1B, CTX3C, CTX4A, epideoxyCTX1B, and 51hydroxyCTX3C were supplied by co-researcher Yasumoto who is same supplier as the lipophilic shellfish toxins. NMR test tubes with 5 mm outer diameters were purchased from Kusano Science Co. (Tokyo, Japan).

Pyridine-d_5 (99.8% deuterium content) was obtained from Merck KGaA (Darmstadt, Germany), and the CRM, 1,4-BTMSB-d_4 (purity 99.8%, expanded uncertainty was 0.5%, k = 2), was from FUJIFILM Wako Pure Chemical Corporation (Osaka, Japan).

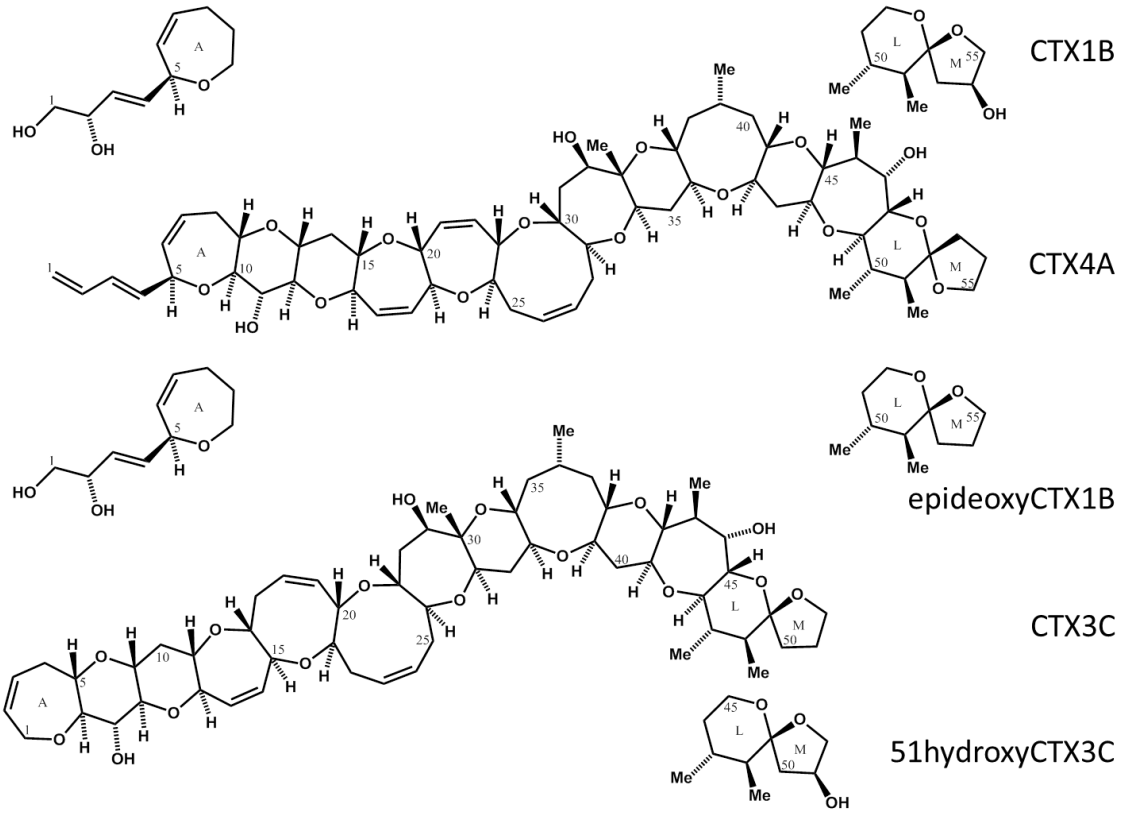

Fig. 7 Structure of CTXs.

CTX1B, Chemical Formula: $C_{60}H_{86}O_{19}$, Molecular Weight: 1111.31; epideoxyCTX1B, Chemical Formula: $C_{60}H_{86}O_{18}$, Molecular Weight: 1095.31; CTX3C, Chemical Formula: $C_{57}H_{82}O_{16}$, Molecular Weight: 1023.25; 51hydroxyCTX3C, Chemical Formula: $C_{57}H_{82}O_{17}$, Molecular Weight: 1039.25; CTX4A, Chemical Formula: $C_{60}H_{84}O_{16}$, Molecular Weight: 1061.29.

2.2.2 Apparatus

The experimental setup was composed of a semi-micro balance (AG285 or MS205DU, Mettler-Toledo, Greifensee, Switzerland), an ultra-micro balance (MSE2.7S, Sartorius AG, Göttingen, Germany), and an NMR spectrometer equipped with a Varian 5-mm indirect probe (Varian NMR System 500, Varian Technologies, Palo Alto, CA, USA).

2.2.3 Determination of the residual proton content in pyridine-d_5

Accurately weighed 1,4-BTMSB-d_4 CRM (1.0197–1.5668 mg) was mixed with pyridine-d_5 (0.77421–0.80378 g) to afford test solutions of 1,4-BTMSB-d_4 CRM (N = 5). The accurate quantity of pyridine-d_5 was pre-determined by weighing the ampule before and after taking out pyridine-d_5. The residual protons of pyridine-d_5 were quantified by comparing the signal intensity with that of CRM.

2.2.4 Preparation of test solutions of CTXs

CTX1B was dissolved in an ampule of pyridine-d_5 to afford test solutions of CTX1B. The accurate amount of pyridine-d_5 (0.79830 g) used for the test solution was determined by weighing with a semi-micro balance. The other CTXs were dissolved in 1 mL of pyridine-d_5 to afford test solutions of CTX. The accurate amount of pyridine-d_5 (1.04616–1.05397 g) used for each test solution was determined by weighing with a semi-micro balance. A 600 µL portion of the test solution was transferred into an NMR test tube for the measurement of the ^{1}H NMR spectrum.

2.2.5 ^{1}H NMR measurements

The relaxation delay was set at six times the longest relaxation time (T_1) of the pyridine signals to recover over 99% of z-magnetization[9]; T_1 was pre-determined by an inversion-recovery test. The following settings were used for the qNMR experiments: irradiation frequency, 499.87 MHz; acquisition time, 4 s; relaxation delay, 60 s; probe temperature, 5 or 25 °C; spectral width, 40 ppm; FID data points, 161,290; number of scans, 8 to 2,560; spinning, off; pre-scans, two times; ^{13}C decoupling, MPF8; pulse angle, 90°; pulse width, 10.4 µs.

2.2.6 Data processing

The data were processed with VnmrJ software ver. 2.3, supplied by the manufacturer (Varian Technologies, Palo Alto, CA, USA). Fourier transformation was performed on 262,144 data points without using window functions. All proton chemical shifts were referenced to a residual proton signal at positions 2 and 6 in pyridine-d_5 at 8.765 ppm. The phase of all spectra was collected manually while observing a spectral line shape. The baseline of spectra was adjusted horizontality, and each signal area ratio was calculated by software functions. An integration range was individually optimized based on the line width of the signals and the space between the signals. The spectra were integrated using the spectral bucketing technique with 0.002-ppm-sized buckets. The area ratio of each signal was calculated by adding all buckets larger than the buckets arising from the baseline (noise level; Fig. 8).

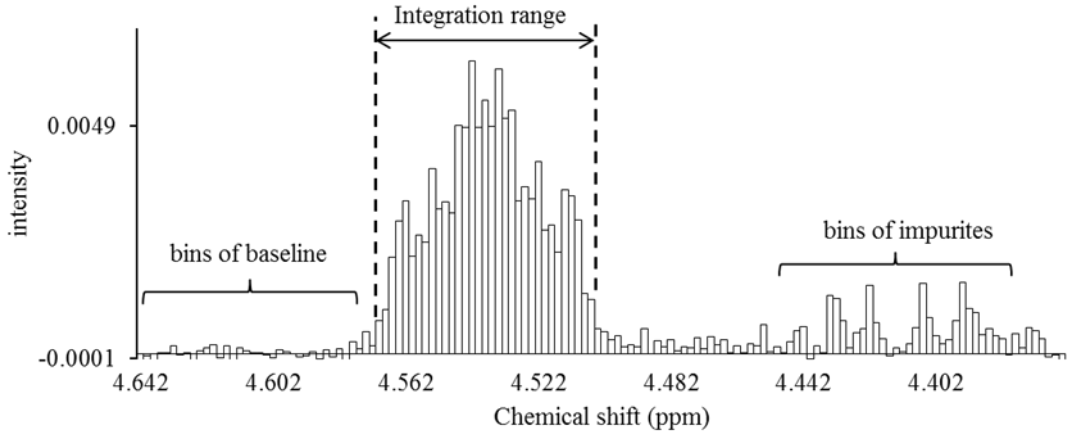

Fig. 8 Signal integration using the spectral bucketing technique.

All spectra were integrated as 0.002-ppm-sized buckets. The area ratio of each signal was calculated by adding all buckets larger than the buckets arising from the baseline. Baseline correction of all spectra was performed by using a software function before performing the integration process. The area ratio of the baseline bucket is desirably close to zero after software baseline correction. If the baseline bucket had a relatively large area ratio, a correction was made by subtracting the area from all buckets to serve as a more precise baseline correction.

2.2.7 Calculation of CTXs content

The quantity of CTXs were calculated by ^{1}H NMR experiments using the residual proton signal of pyridine-d_5 as the IS, based on the following Equation (3):

$$Value_A = \frac{I_A}{I_{IS}} \times \frac{N_{IS}}{N_A} \times \frac{M_A}{M_{IS}} \times W_{IS} \times Q_{IS} \quad (3)$$

where $Value_A$ is the quantity of CTX (weight); I_A is the area ratio of each individual signal arising from CTX; I_{IS} is the area ratio of the residual proton of pyridine-d_5; N_{IS} is the number of protons of the residual proton of pyridine-d_5; N_A is the number of protons of CTX; M_A is the mole weight of CTX; M_{IS} is the mole weight of the residual proton of pyridine-d_5; W_{IS} is the weight of pyridine-d_5; and Q_{IS} is the quantity of the residual proton of pyridine-d_5.

2.3 Results

2.3.1 Determination of the residual proton content of pyridine-d_5 and purity calculation

The ^{1}H NMR spectrum of pyridine-d_5 (Fig. 9) exhibited three residual proton signals arising from H-2 and H-6 (8.76 ppm), H-4 (7.61 ppm), and H-3 and H-5 (7.24 ppm). The residual proton content in pyridine-d_5 was calculated by ^{1}H NMR experiments using 1,4-BTMSB-d_4 as the IS, based on the following Equation (4):

$$Value_A = \frac{I_A}{I_{IS}} \times \frac{N_{IS}}{N_A} \times \frac{M_A}{M_{IS}} \times \frac{W_{IS}}{W_A} \times P_{IS} \quad (4)$$

where $Value_A$ is the quantity of the residual proton in the pyridine-d_5; I_A is the area ratio of each individual (define ratio) signal arising from the residual proton; I_{IS} is the area ratio of the IS; N_{IS} is the number of protons of the IS; N_A is the number of protons of the residual proton; M_A is the mole weight of the residual proton, calculated by employing C_5H_5N as the chemical formula; M_{IS} is the mole weight of the IS; W_{IS} is the weight of the IS; W_A is the weight of the pyridine-d_5; and P_{IS} is the purity of the IS.

The quantity of each residual proton signal in pyridine-d_5 calculated was determined to be

0.149%, 0.159%, and 0.153%, respectively. Those residual proton signals showed good repeatability (RSD ranged from 0.30 to 0.33%) between the content of five ampoules, indicating the validity of the signals as ISs. In the same production lot of ampoules, the residual proton of pyridine-d_5 was stably included in a fixed amount. Thus, the use of the same lot of pyridine-d_5 ampoules as an IS solution was enabled. On the other hand, the dispersion between the three signals was as large as 3.1% RSD, and it was considered that the deuterium content differs for each position of pyridine. The residual proton amount was not averaged among the signals and was used as an individual value.

The pre-calibrated pyridine-d_5 ensures an ability to trace an absolute quantity of the CTX standards to the SI units. Of the three signals of the residual protons, two signals at a higher field (7.61 and 7.24 ppm) were overlapped with the hydroxy protons of 11-OH and 47-OH in CTX1B or 7-OH and 44-OH of CTX3C and thus judged unsuitable for use as the IS. Being free of contamination, the signal at 8.43 ppm (H-2, H-6) was judged appropriate for the calculation (Fig. 9).

2.3.2 Quantification of respective CTXs

The ^{1}H NMR spectra of CTX1B, epideoxyCTX1B, and CTX4A are shown in Fig. 10. The signals, though congested, were assignable based on the reference[37,38]. Apparently, the signals suitable for quantitative use are limited to a few arising from the protons of olefins and hydroxyls. They are moderately well separated from the congested signals of the protons on the skeletal structures. The separation between the olefin and hydroxyl proton signals was best achieved by measuring at 5 °C. The signals B and D, characteristic to the 3-butene-diol side-chain of the CTX1B and epideoxyCTX1B, feature narrow line widths and sufficient intensity to make them suitable for calculation. Calculations based on these signals placed the content at 0.14 mg (0.2% RSD) for CTX1B and 0.06 mg (0.5% RSD) for epideoxyCTX1B. Similarly, signals A and C, arising from 2-OH located in the lower-magnetic field, had narrow

line widths and adequate intensity. The CTX content calculated therefrom was almost a complete match with those from the aforementioned signals B and D. The accuracy of the quantification was thus supported (Table 3). The protons that produced signals A, B, C, and D do not belong to the polyether rings but to the side-chains. Unlike the protons on the cyclic rings, the protons on the side-chain are less susceptible to the conformational changes of the skeletal rings and, therefore, the broadening of the signals is reduced. The characteristic multiple (multiplet) signals, F and G, arising from the 1,3-diene of the side chain in CTX4A also feature narrow line widths suitable for the CTX4A quantification. However, the multiple line shape resulted in low signal intensity and inevitably led to a large dispersion of the quantitative value (0.07 mg; 2.3% RSD), as compared with the value obtained on an equivalent concentration of epideoxyCTX1B (0.06 mg; 0.5% RSD).

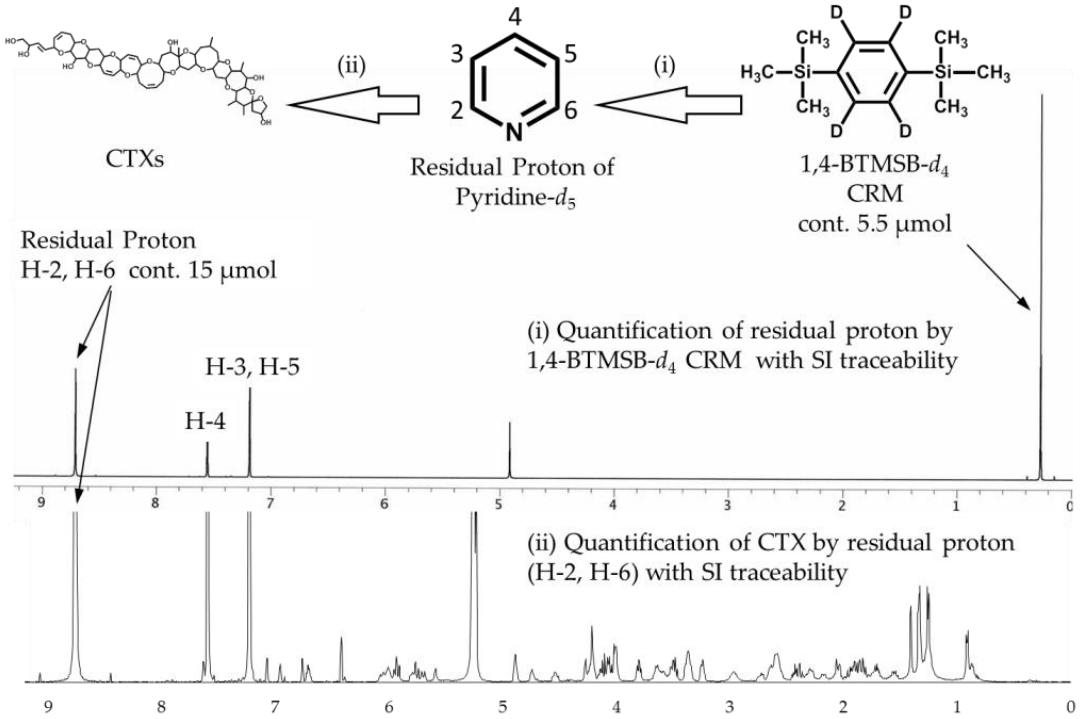

Fig. 9 Scheme for the indirect determination of CTX and for keeping the traceability to SI using qNMR by employing volatile substances as the IS.

The upper spectrum exhibits the residual proton signals of pyridine-d_5, and an IS signal of 1,4-BTMSB-d_4. The lower spectrum exhibits signals of CTX and an IS signal of residual proton. The signal intensity of the residual proton contained in the CTXs/pyridine-d_5 solution was approximately 30 when the signal of 1,4-BTMSB-d_4 was taken as 100.

Table 3 The quantities of CTX1B, epideoxyCTX1B, and CTX4A.

Compounds	Signals	Assignment of Signals	S/N	Signal Intensity	Quantitative Value (mg)
CTX1B	A	Hydroxyl group 2	28	-	0.1374 ± 0.0012
	B	Olefin 3, 4	68	0.25	0.1381 ± 0.0003
epideoxyCTX1B	C	Hydroxyl group 2	11	-	0.0590 ± 0.0017
	D	Olefin 3, 4	48	0.11	0.0586 ± 0.0003
CTX4A	E	Hydroxyl group 47	14	-	0.0832 ± 0.0007
	F	1,3-diene 3	20	0.075	0.0794 ± 0.0018
	G	1,3-diene 2	20	-	0.0743 ± 0.0017

The quantitative values were calculated using signals A to G in Fig. 10. The signal intensity was expressed as a signal of 1,4-BTMSB-d_4 as 100. Signals B of CTX1B, D of epideoxyCTX1B, and F and G of CTX4A were used for the final quantification.

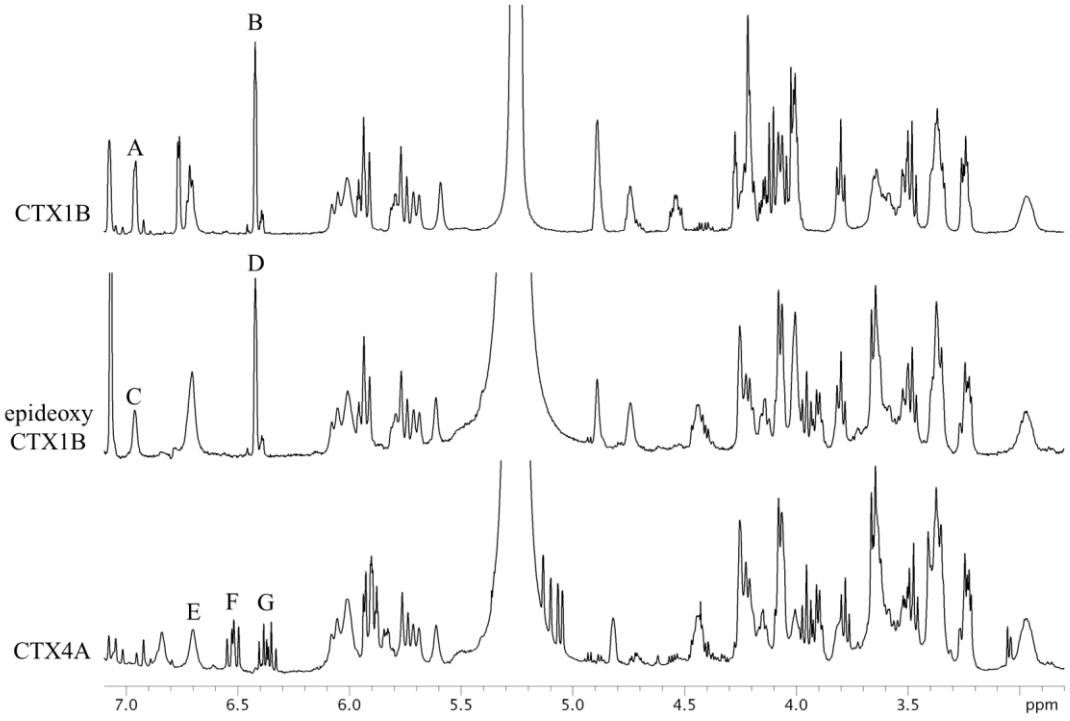

Fig. 10 The ^{1}H NMR spectra of CTX1B, epideoxyCTX1B, and CTX4A.

The parameters and conditions for the measurements are set as follows: CTX1B, instrument; Varian NMR System 500; data point, 65,536; pre-scans, two times; number of scans, 512 times; relaxation delay, 60 s; temperature, 5 °C; acquisition time, 4 s. For epideoxyCTX1B; instrument, Varian NMR System 500; data point, 65,536; pre-scans, two times; number of scans, 2048 times; relaxation delay, 60 s; temperature, 5 °C; acquisition time, 4 s. For CTX4A; instrument, Varian NMR System 500; data point, 65,536; pre-scans, two times; number of scans, 3072 times; relaxation delay, 60 s; temperature, 5 °C; acquisition time, 4 s.

CTX3C and 51hydroxyCTX3C lack the side chain useful for the quantification of the aforementioned CTXs. All the protons were tested for suitability for quantitative determination (Table 4). The CTX3C content was calculated to be 0.41 mg (0.9% RSD) using the signal H (44-OH), as shown in Fig. 11. The hydrogen-bond formation of hydroxyl protons gave rise to a wide variety of line shapes. Nevertheless, the signals were narrow and sufficiently strong and produced values more accurate than those obtained from other signals (I and J). Since the 44-OH signal of 51hydroxyCTX3C was observed to have significant overlaps with impurities, the calculation was performed using the methylene proton signals K (H-17) positioned at 2.9 ppm. The amount of 51hydroxyCTX3C was calculated to be 0.013 mg (1.5% RSD), but the author concluded that the 500-MHz NMR instrument does not provide enough sensitivity to the small sample of only one-tenth the quantity of CTX1B. Therefore, the author carried out measurements using an 800-MHz NMR instrument equipped with a cryogenically-cooled probe. The quantities of 51hydroxyCTX3C could be determined down to 0.011 mg using the amplified signals L (H-38, 42), M (H-22, 25), and N (H-17), as shown in Fig. 12.

Table 4 The quantities of CTX3C and 51hydroxyCTX3C.

Compounds	Signals	Assignment of Signals	S/N	Signal Intensity	Quantitative Value (mg)
CTX3C	H	Hydroxyl group 44	81	0.40	0.4060 ± 0.0038
	I	Olefin 2, 3, 13, 14, 18, 19, 23, 24	-	-	0.4408 ± 0.0018
	J	17-H	37	-	0.4243 ± 0.0067
51hydroxyCTX3C	K	17-H	<10	0.013	0.0134 ± 0.0002
	L	38, 42-H	25	-	0.01089
	M	22, 25-H	10	-	0.01230
	N	17-H	10	-	0.01085

The quantitative values were calculated using the signals H to K in Fig. 11 and L to N in Fig. 12. The signal intensity was expressed as a signal of 1,4-BTMSB-d_4 as 100. Signals H of CTX3C and L to N of 51hydroxyCTX3C were used for the final quantification.

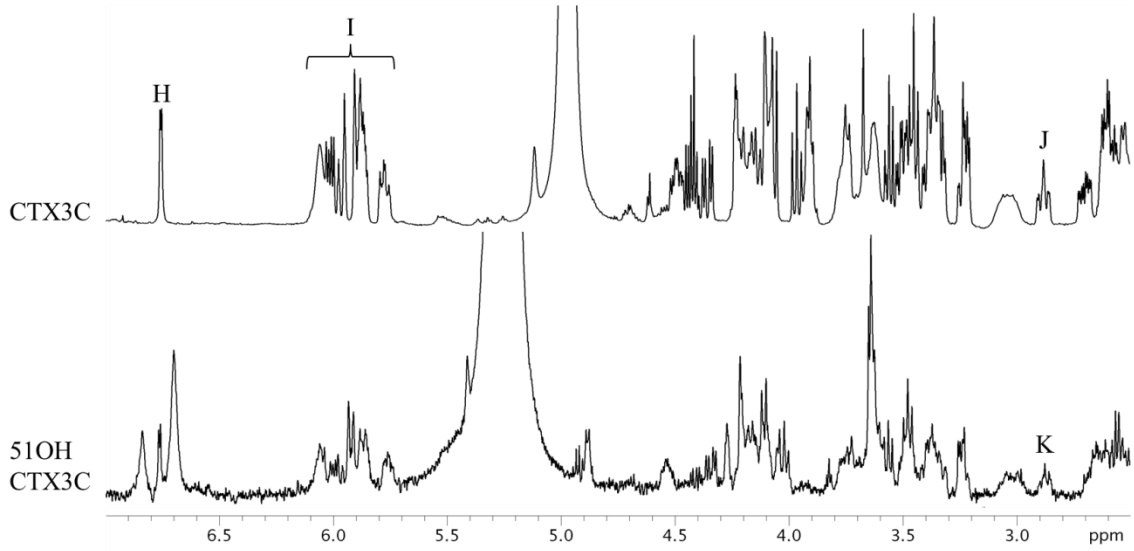

Fig. 11 The ^{1}H NMR spectra of CTX3C and 51hydroxyCTX3C.

The parameters and conditions for the measurements are given below. CTX3C: Instrument, Varian NMR System 500; data point, 65,536; pre-scans, two times; number of scans, 512 times; Relaxation delay, 60 s; temperature, 25 °C; Acquisition time, 4 s. 51hydroxyCTX3C: Instrument, Varian NMR System 500; data point, 65,536; pre-scans, two times; number of scans, 1280 times; Relaxation delay, 60 s; temperature, 5 °C; Acquisition time, 4 s.

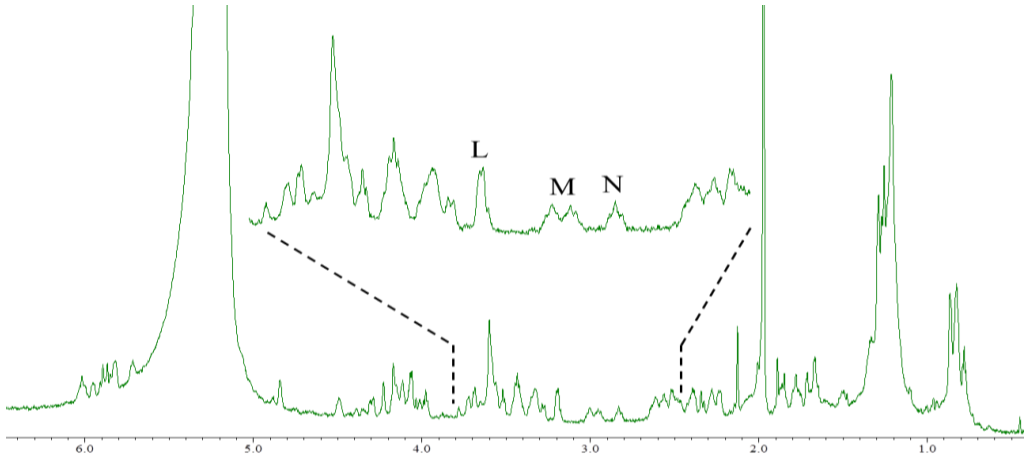

Fig. 12 The ^{1}H NMR spectrum of 51hydroxyCTX3C using high magnetic field NMR.

Instrument, JNM-ECA800 with cryogenically cooled probe (Jeol Ltd., Tokyo, Japan); irradiation frequency, 800.14 MHz; data point, 65,536; pre-scans, 32 times; number of scans, 512 times; Relaxation delay, 56.7 s; temperature, 5 °C; Acquisition time, 3.3 s.

2.4 Discussion

Since ciguatera fish poisoning is the largest category of food poisoning of natural etiology, it has stimulated scientists to test and propose various testing methods. The use of anti-toxin

antibodies faces problems arising from the abundance of structurally variant congeners. The functional assay based on the specific binding of the toxins to the voltage-dependent sodium channel uses a radio-active ligand, which requires strict regulatory control. The function-based-cytotoxicity assay provides the highest sensitivity. However, the practical merit of the method awaits future validation on various fish species. The rapid progress in LC/MS analysis promises its potential due to its sensitivity and accuracy. In all analytical methods, including LC/MS, the use of a reliable standard is imperative. Nevertheless, the preparation of CTXs standards is a great challenge for two reasons. First, the availability of CTXs is extremely limited because most CTXs are the metabolites of fish and unavailable in algal cultures. The second problem is related to the technology itself. Containing 82 to 86 protons, CTXs produce congested and partially overlapped NMR signals. Many flexible rings in the structure allow multiple conformers that lead to the broadening of signals. Despite these difficulties, the present qNMR method successfully achieved the quantification of CTX1B, epideoxyCTX1B, CTX4A, CTX3C, and 51hydroxyCTX3C by choosing the proper signals. The olefinic protons arising from side chains were preferred to those on the polyether rings to avoid broadened signals, enabling quantification down to 0.06 mg (epideoxyCTX1B) with high accuracy. The absence of the side-chain in CTX3C and its analogues made us newly select other protons. After vigorous testing of every signal, the author found the signals arising from 44-OH and H-17 to possess the necessary quality for qNMR. The quantity of 51hydroxyCTX3C amounted to only 1/40 of CTX3C, which was too small to produce valid signals on a 500-MHz instrument. The high field 800-MHz NMR instrument equipped with a cryogenically-cooled probe could quantify CTXs down to 0.01 mg. CTXs thus quantified are planned to be used as standards in LC/MS measurements.

After the measurement of the NMR spectra, each CTX reference standard solution was individually prepared by diluting the CTX test solution with methanol. The CTX reference standard solution was dispensed in small aliquots into small glass vials, and the solvent was

removed by a drying operation. To prevent the nonspecific adsorption of CTXs onto the glass wall surface, a very small amount of ethanol was added to each vial.

2.5 Conclusion

The author achieved quantification of CTX1B, epideoxyCTX1B, CTX4A, CTX3C, and 51hydroxyCTX3C by employing qNMR method. Despite the congestion and partial overlap of the spectra, CTXs could be quantified by choosing proper signals. The protons on the side chains were preferred to those on the rings to avoid broadened signals. A 500 MHz NMR spectrometer could quantify CTXs above 50 μg. The 800 MHz spectrometer was able to measure even a small amount of 11 μg 51hydroxyCTX3C. The use of the residual protons of pyridine-d_5 as the ISs made it unnecessary to remove the IS after measurement. Thus, the risk of contamination due to conventional CRM was avoided and the overall manipulation was simplified. The author successfully achieved producing the CTXs reference standard for LC/MS measurement based on this study results.

Chapter 3

Quantitative Phosphorus Nuclear Magnetic Resonance Method for Individual and Concomitant Determination of Phospholipid Classes in Polar Lipid Samples

3.1 Introduction

Phospholipids are polar lipids with amphiphilic and bilayer-forming characteristics, and are widely used as additives in foods, cosmetics, or dietary supplements. Furthermore, phospholipids form liposomes in aqueous solution, which has received much attention as a medium for transporting pharmaceutical ingredients.

The properties of the resultant emulsion and bilayer are strongly dependent on the phospholipid species and concentration. Consequently, an accurate determination of phospholipid quantity is accordingly required, and particularly required for individual quantification of phospholipid classes. Conventionally, a laborious 2D-TLC method has been used for phospholipid quantification, in which phospholipid classes are individually separated by 2D-TLC, extracted from the TLC plate, and then determined colorimetrically using molybdic acid[39, 40]. This method is reliable, but requires careful operation. Recently, an HPLC method using an ELSD[41–43] that achieves excellent separation of the phospholipid classes has been widely adopted. Unfortunately, the dynamic range of this method is relatively narrow owing to the nonlinear response of the detector[44].

In contrast, phosphorus nuclear magnetic resonance (^{31}P NMR)[45] can realize the mutual separation of phospholipid classes in a relatively easy operation. NMR provides well-separated signals of individual phospholipid classes with chemical shifts based on structural differences in hydrophilic groups. Furthermore, as the ^{31}P NMR signal area ratio represents the molar ratio of phosphorus nuclei, this method can directly determine the molar ratio of phospholipid classes in

samples without using a reference standard. In previously reported ^{31}P NMR quantification methods, phospholipids have been dissolved in a mixed solvent (chloroform–methanol) containing a limited amount of aqueous ethylenediaminetetraacetic acid (EDTA) solution to improve the spectrum line width[46,47]. In other methods, a homogeneous test solution was obtained by using cholic acid as a surfactant. Cholic acid forms tiny micelles in aqueous solution that incorporate phospholipids and suppress the liposome formation by phospholipids. As a result, ^{31}P NMR of an aqueous solution of phospholipids containing cholic acid and EDTA gives highly resolved signals[48–50].

Recently, ^{1}H NMR that enables accurate quantification, known as qNMR, has become a widely used method. In particular, the AQARI or equivalence method, using CRM as an IS, has been successfully used to precisely determine the quantity and purity of low-molecular-weight organic compounds.

In the present research, the phospholipid quantification method by ^{31}P NMR was carefully optimized using an aqueous sodium cholate–EDTA solution system with the presence of phosphoserine (PSER) as a certified reference material, and with controlling the pH of the sample in order to separate and quantify at most phospholipid classes effectively and concomitantly. The improved method was successfully applied to the absolute quantification of phospholipids in commercially distributed soybean lecithin and dietary foods. Furthermore, the results of the present ^{31}P NMR method were verified by comparison with the AQARI-based ^{1}H NMR method using 1,4-BTMSB-d_4 CRM. AQARI is an absolute quantitative method that can obtain quantitative values with SI traceability and is highly reliable, with sufficiently advanced verification. The quantified results of phospholipid classes from ^{31}P NMR were also compared with those of conventional molybdenum blue colorimetry and 2D-TLC methods. The present method recognized the total phospholipid contents of polar lipids, and were in good agreement with those obtained by molybdenum blue colorimetry. However, the quantitative values for individual phospholipid classes were varied depending on their content between 2D-TLC and

^{31}P NMR.

3.2 Experimental

3.2.1 Materials and chemical reagents

Soybean phosphatidylethanolamine (PE), soybean phosphatidylinositol (PI), soybean lysophosphatidylinositol (LPI), egg yolk PE, egg yolk phosphatidic acid (PA), egg yolk lysophosphatidylcholine (LPC), egg yolk lysophosphatidylethanolamine (LPE), and synthetic 2-lyso-oleoylphosphatidic acid (2-LOPA) were purchased from Sigma-Aldrich Co. LLC. (St. Louis, MO, USA). Soybean phosphatidylcholine (PC) and egg yolk sphingomyelin (SM), and synthetic phospholipids dioleoylphosphatidylcholine (DOPC), dioleoylphosphatidylserine (DOPS), distearoylphosphatidic acid (DSPA), distearoylphosphatidylethanolamine (DSPE), palmitoyloleoylphosphatidylethanolamine (POPE), distearoylphosphatidylglycerol (DSPG), and palmitoyloleoylphosphatidylglycerol (POPG), were purchased from NOF Corporation (Tokyo, Japan). Polar lipids extracted from soybean, porcine brain, and yeast were obtained from Avanti Polar Lipids, Inc. (Alabaster, AL, USA). Phospholipid samples soy lecithin 1 (95 g of phospholipid per 100 g, including 28 g of PC) and soy lecithin 2 (1.2 g of phospholipid per soft capsule, including 0.18 g of PC) were purchased from an internet store (https://www.amazon.co.jp/). Phosphatidylserine (PS) dietary supplement food 1 (containing 50 mg of PS and 30 mg of PC per hard capsule) and PS dietary supplement food 2 (containing 100 mg of PS per soft capsule) were also purchased from the same internet store. The PSER traceable reference material (TRM, purity 99.5%, expanded uncertainty was 0.9%, k = 2) and the 1,4-BTMSB-d_4 CRM (purity 99.8%, expanded uncertainty was 0.5%, k = 2) were obtained from FUJIFILM Wako Pure Chemical Corporation (Osaka, Japan). Sodium cholate was purchased from Tokyo Chemical Industry Co., Ltd. (Tokyo, Japan). EDTA 2Na was obtained from Dojindo Laboratories (Kumamoto, Japan). Deuterium oxide (99.9% deuterium content) was obtained from Merck KGaA (Darmstadt, Germany). Deuterated dichloromethane (99.8%

deuterium content) was obtained from Kanto Chemical Co., Inc. (Tokyo, Japan). Silica gel 60 HPTLC plates (size 10 x 10 cm) were obtained from Merck KGaA (Darmstadt, Germany). And NMR test tubes with a 5-mm outer diameter were purchased from FUJIFILM Wako Pure Chemical Corporation (Osaka, Japan).

3.2.2 Apparatus

Phospholipids and samples were weighed using a semi-micro balance (MS205DU, Mettler–Toledo, Greifensee, Switzerland). PSER and 1,4-BTMSB-d_4 were precisely weighed using an ultra-micro balance (MSE2.7S, Sartorius AG, Göttingen, Germany). ^{1}H NMR spectra were measured using an NMR spectrometer equipped with a 5-mm indirect probe (Varian NMR System 500, Varian Technologies, Palo Alto, CA, USA). ^{31}P NMR measurements were performed using a JNM-ECA500II spectrometer (JEOL Ltd., Tokyo, Japan) equipped with a 5-mm FG/RO Digital Auto Tune Probe.

3.2.3 ^{31}P NMR measurements

A surfactant solution (20%) was prepared by dissolving sodium cholate (20 g) in deuterium oxide (100 mL). EDTA 2Na (2.5 g) was dissolved in Tris–HCl buffer (25 mL, 1 M, pH 7.0) to prepare an EDTA solution (100 mg/mL). A mixture of accurately weighed PSER (20 mg) and EDTA solution (2 mL) was made up to 20 mL by adding Tris–HCl (1 M, pH 7.0) and used as an IS solution (1 mg/mL). The synthetic phospholipid was dissolved in the surfactant solution at concentrations ranging from 0.5 to 2%. Soybean lecithin powder was dispersed in the surfactant solution (1 mL) to give total phospholipid contents ranging from 0.4 to 6.6%. The IS solution (1 mL) was then added, and the mixture was shaken for 1 h at 50 °C. Solutions of PS dietary supplements 1 and 2 containing PS were prepared using the same procedure as for the soya lecithin powder, but without their capsules. The obtained mixture of phospholipid extract and the IS was a cloudy liquid that was then centrifuged at 15,000 rpm. The pH of the obtained

supernatant was adjusted to 6.90 ± 0.04 using 1 M NaOH or 1 M HCl solutions and then used for ^{31}P NMR measurements. ^{31}P NMR spectra were measured using the following conditions: irradiation frequency, 202 MHz; acquisition time, 5.453 s; probe temperature, 30 °C; spectral width, 80 ppm; FID data points, 65,536; spinning, 15 Hz; pre-scans, 4; ^{1}H decoupling, Waltz16; pulse angle, 90°; pulse width, 14.8 μs.

3.2.4 Absolute quantification of DOPC by ^{31}P NMR and ^{1}H NMR

DOPC (20.21–20.89 mg) and PSER (1.12–1.67 mg) as IS were accurately weighed and dissolved in the surfactant solution (2 mL) to prepare a test solution. This test solution was used for ^{31}P NMR measurement under the conditions mentioned above (section 3.2.3). Another test solution was prepared by dissolving accurately weighed DOPC (20.17–20.26 mg) and 1,4-BTMSB-d_4 (1.00–1.01 mg) as IS in deuterated dichloromethane (0.9 mL). This test solution was used for ^{1}H NMR measurement. The ^{1}H NMR relaxation delay expected to recover over 99.9% of z magnetization was set to seven times the longest T_1 of ^{1}H signals[9]. T_1 was determined using an inversion-recovery experiment. ^{1}H NMR spectra were measured under the following optimized conditions: irradiation frequency, 500 MHz; acquisition time, 4 s; relaxation delay, 40 s; probe temperature, 25 °C; spectral width, 40 ppm; FID data points, 161,290; number of scans, 8; spinning, off; pre-scans, 2; ^{13}C decoupling, MPF8; pulse angle, 90°; pulse width, 10.4 μs.

3.2.5 Calculation of phospholipid quantity

The purity of DOPC was determined from ^{1}H and ^{31}P NMR spectra. The purity value of DOPC was determined by ^{1}H NMR with 1,4-BTMSB-d_4 as IS using Equation (5). The purity (P_{IS}) of 1,4-BTMSB-d_4 was traceable to the SI, therefore traceability was inherited in the purity (P_A) of DOPC obtained by calculation. Quantitative values were calculated from ^{31}P NMR using PSER as the IS traceable to the SI.

$$P_A = \frac{I_A}{I_{IS}} \times \frac{N_{IS}}{N_A} \times \frac{M_A}{M_{IS}} \times \frac{W_{IS}}{W_A} \times P_{IS} \quad (5)$$

where P_A is the purity of DOPC (%); I_A is the area ratio of the DOPC signal; I_{IS} is the area ratio of the IS; N_{IS} is the number of protons or phosphorus atoms in the IS; N_A is the number of protons or phosphorus atoms in DOPC; M_A is the molecular weight of DOPC; M_{IS} is the molecular weight of the IS; W_{IS} is the weight of IS used (g); W_A is the weight of DOPC used (g); and P_{IS} the purity of the IS (%).

The molar amount of phospholipid in the sample was determined from the ^{31}P NMR spectrum of the test solution. The molar amounts of individual phospholipid classes were determined from the ^{31}P NMR spectrum of the test solution with PSER as IS using Equation (6). Furthermore, the contents (%) of individual phospholipid classes were calculated using Equation (7), assuming that fatty acids bind to the *sn*-1 and *sn*-2 positions of the phospholipids as stearic acid.

$$Mol_A = \frac{I_A}{I_{IS}} \times Mol_{IS} \quad (6)$$

$$Value_A = \frac{I_A}{I_{IS}} \times \frac{N_{IS}}{N_A} \times \frac{M_A}{M_{IS}} \times \frac{W_{IS}}{W_A} \times P_{IS} \quad (7)$$

where Mol_A is the molar amount of the phospholipid; Mol_{IS} is the molar amount of the IS; $Value_A$ is the quantity (%) of phospholipid; I_A is the area ratio of the phospholipid; I_{IS} the area ratio of PSER; N_{IS} is the number of phosphorus atoms in PSER; N_A is the number of phosphorus atoms in the phospholipid; M_A is the molecular weight of the phospholipid; M_{IS} is the molecular weight of PSER; W_{IS} is the weight of PSER; W_A is the weight of the polar lipid sample; and P_{IS} is the purity (%) of PSER.

3.2.6 Colorimetric quantification of total phospholipids using molybdenum blue

The total phospholipids contained in polar lipid samples of soybean, porcine brain, and yeast were quantified by a colorimetric method using molybdenum blue. Specific procedures are listed in standard method 2.4.11-2013 (JOCS 2.4. 11-2013)[51] from Standard Methods for the Analysis of Fats, Oils and Related Materials, which is the official oil analysis method in Japan established by Japan Oil Chemists' Society. The sample amounts collected were 112.1 mg of soybean polar lipid, 99.0 mg of porcine brain polar lipid, and 99.0 mg of yeast polar lipid. Each sample was taken up in chloroform (50 mL), fractionated into 2-mL crucibles, and the solvent was then removed by blowing with nitrogen gas before testing.

3.2.7 Quantification of individual phospholipids using 2D-TLC

The separation and classification of phospholipids by 2D-TLC was conducted according to standard method 4.3.3.1-1996 (JOCS 4.3.3.1-1996)[40] from Standard Methods for the Analysis of Fats, Oils and Related Materials. However, the polar lipids extracted from samples were prepared by the alternative procedure described in Section 3.2.6 (18.87–19.88 mg of soybean polar lipid, 15.95–16.34 mg of porcine brain polar lipid, and 16.76–17.07 mg of yeast polar lipid were used) and then dissolved in chloroform to give 2 mg/mL polar lipid solutions. The polarlipid solutions (20 μL) were separated by 2D-TLC for collecting of individual phospholipid using solvent 1 and 2, with the amount of phosphorus measured and the composition ratio calculated for each phospholipid class. Solvent 1 contained tetrahydrofuran, acetone, methanol, and water (50:20:40:8, *v/v*), while solvent 2 contained chloroform, acetone, methanol, acetic acid, and water (50:20:10:15:5, *v/v*). Each phospholipid spot was clearly visualized by the Dittmer reagent and individually scraped from Silica gel 60 HPTLC plate and transferred into the digestion tube. These recovered phospholipids were quantified by the molybdenum blue method according to Section 3.2.6. Quantitative values of individual phospholipid classes were calculated by multiplying the total phospholipid amount

obtained (see Section 3.2.6) by the composition ratio for each class.

3.3 Results and Discussion

3.3.1 Determination of DOPC quantity by ^{1}H NMR

A typical ^{1}H NMR spectrum of DOPC is shown in Fig. 13. This experiment was conducted as three parallel tests, and the quantitative values obtained are shown in Table 5. Signals A–I, derived from the partial structure of DOPC (oleic acid, choline, and glycerol), were observed in the spectrum. Among these signals, signal A was not used for the quantitative calculation because it overlapped with the solvent signal (dichloromethane). The purity was calculated using signals B–I, which were separated by sufficient intervals, and tended to be higher when higher-field signals were used in the calculations instead of low-field signals. The values were particularly high when using signals G–I, assigned to methyl and methylene groups of fatty acid chains. However, signal D of the *N*-methyl group of choline was a strong single peak with a narrow line width and no interference from any impurities. Signal D was accordingly considered the most reliable signal for determining the true value. Consequently, the purity of DOPC was determined as 99.1 ± 0.3% by ^{1}H NMR.

3.3.2 Optimization of phospholipid chemical shifts

In the ^{31}P NMR spectra of phospholipids, the phosphate chemical shift was affected by the pH of the test solution. Particularly significant chemical shift changes were observed for PE, PS, and their lyso forms[50]. Further improvements in the mutual separation of each phospholipid class would be possible through pH control. However, under alkaline conditions, acyl group hydrolysis and lysophospholipid formation would be accelerated. Furthermore, sodium cholate precipitation was anticipated under acidic conditions. Consequently, the conditions were optimized to pH 6.90 ± 0.04 at 30.0 ± 0.1 °C (Table 6). No appreciable change (± 0.001 ppm) was observed in the chemical shifts of DOPC, DOPS, DSPG, SM, and DSPE when varying the

concentration from 0.1 to 1%, or in that of DSPE at concentrations of 0.025–0.5% under the optimal fixed pH and temperature. However, the chemical shifts of DSPA and PSER showed relatively large fluctuations (± 0.02 ppm) at concentrations of 0.025–0.5% and 0.05%, respectively. LPI was difficult to quantify using this condition since 1-LPI was overlapped 2-LPC and 2-LPI was overlapped PE. However, because the LPI content in the polar lipid samples was very small, the quantitative values of PE and 2-LPC should not come into significant problem. Except for SM, the phospholipids from natural products, including egg yolk and soybean, showed signals with multiple apexes owing to the heterogeneity in fatty acid composition. Furthermore, the PC signal from soybean comprised two peaks[52], the resolution of which decreased at concentrations of 1% or higher.

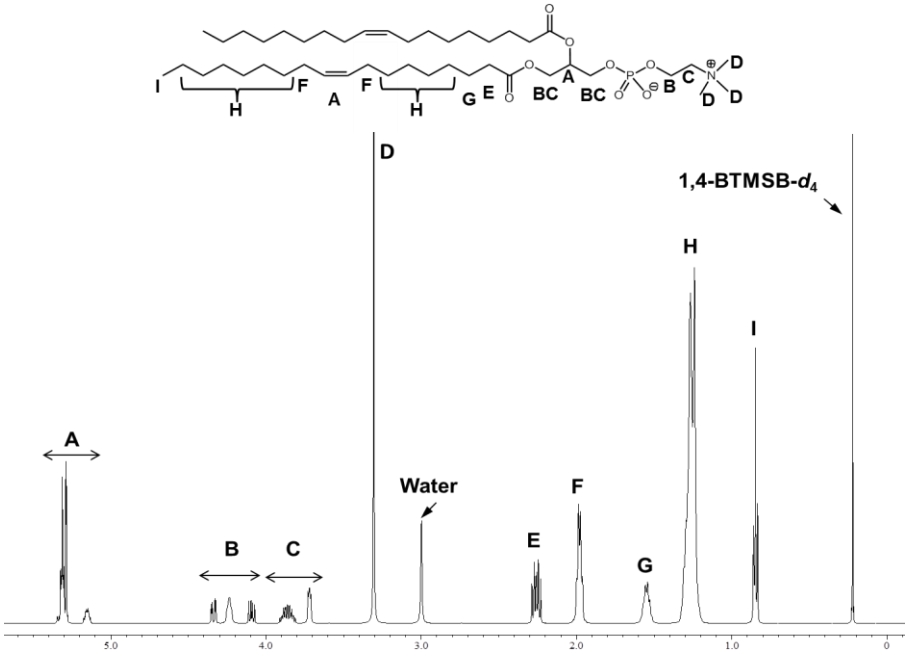

Fig. 13 ^{1}H NMR spectrum of DOPC.

DOPC (20 mg) in CD_2Cl_2 (0.9 mL) with 1,4-BTMSB-d_4 (1 mg) as IS. The parameters and conditions for the measurements are set as follows: instrument; Varian NMR System 500; data point, 161,290; pre-scans, 2; number of scans, 8 times; relaxation delay, 40 s; probe temperature, 25 °C; acquisition time, 4 s. Signal A to C are composed of multiple signals.

Table 5 Calculated purity of DOPC using ^{1}H NMR (N = 3).

Signals	S/N ratio	Number of nuclei	Purity (%)	SD (%)
B	1100	4	99.1	0.3
C	1400	4	99.1	0.3
D	22000	9	99.1	0.3
E	2500	4	99.4	0.4
F	4600	8	99.2	0.3
G	1600	4	100.4	0.7
H	15000	40	99.6	0.2
I	11000	6	99.7	0.1
1,4-BTMSB-d_4	19000	18	-	-
Average	-	-	99.4	0.3

Table 6 ^{31}P Chemical shifts of phospholipid classes at pH 6.9.

Phospholipid	Chemical shift (ppm)	Phospholipid	Chemical shift (ppm)
DOPC	–0.091	DSPE	0.508 ± 0.001
PC from soy	–0.070, –0.090	SM from egg yolk	0.541 ± 0.001
PI from soy	0.059	DHSM from egg yolk	0.638
1-LPC from egg yolk	0.208	1-LPE from egg yolk	0.791
DOPS	0.250 ± 0.001	2-LPE from egg yolk	0.930
1-LPI from soy	0.385	POPG	0.987
2-LPC from egg yolk	0.386	DSPG	1.000
POPE	0.486	PA from egg yolk	3.844
PE from egg yolk	0.471, 0.487	DSPA	3.903 ± 0.016
PE from soy	0.473, 0.486	2-LOPA	4.464
2-LPI from soy	0.498	PSER	4.543 ± 0.017

DHSM is dihydrosphingomyelin.

3.3.3 Measurement of relaxation time to determine pulse interval time

SI-traceable PSER was used in the present study as a reference standard material for quantification by ^{31}P NMR. For the precise quantification of phospholipids, it is important to obtain an accurate area ratio from signals resulting from the phospholipids and internal standard PSER. Pulse interval time is among the most important parameters for determining the area of an NMR signal accurately. The T_1 of the focusing signal was first measured and then used to calculate an appropriate pulse interval time to be employed. Validation was conducted using three sample categories: (i) DOPC, DOPS, and SM as synthetic high-purity phospholipids; (ii) soy lecithins 1 and 2 as polar lipids extracted from soybean, which are mixtures of phospholipids; and (iii) PS dietary supplement foods 1 and 2, which contain various components other than phospholipids. Samples from each category were dissolved in the surfactant solution and T_1 parameters were measured using the reverse recovery method (Table 7). The T_1 of PC and PS was approximately 0.8–1.1 s, regardless of the molar ratio of cholic acid, the total phospholipid content, and the type of sample. Although the T_1 of PI, PE, and LPC tended to increase at a lower molar ratio of total phospholipids to surfactant, it remained below 2 s. SM from egg yolk, which was highly pure, seemed to have T_1 values similar to those of phospholipids such as PC. However, PA showed a longer T_1 of 1.6–1.7 s, which was different to those of other phospholipids, even when the test solutions contained rather higher phospholipid molar ratio to the surfactant. As the content of PA in the sample was lower than that of other phospholipids, its T_1 could not be measured. However, it was estimated that corresponding T_1 was in the range of approximately 1.5–2.5 s. In contrast, the T_1 of PSER was significantly different to that of other phospholipids, at 1.3–4.3 s depending on the molar ratio to phospholipid. At higher phospholipid concentrations, the T_1 values of phospholipid[53] and PSER became shorter. As the aggregation number of sodium cholate is reportedly as low as 4[54] at 20–25 °C, the ratio of soy lecithin 1 to surfactant in the experiment of 4.3:1 implied that one lecithin molecule was incorporated into a small micelle formed by four sodium cholate species

(Table 7). Therefore, a further increase of the ratio of phospholipid to surfactant should be avoided.

Using the same solution of DOPC used to measure T_1 in Table 7, ^{31}P NMR spectra were obtained by changing the pulse interval time from 0.2 to 20 s in seven steps to compare the area ratio between DOPC and PSER signals. The area of DOPC increased slightly until the pulse interval time reached 1 s, which was close to T_1, and decreased thereafter (Fig. 14). Furthermore, for PSER, the signal area ratio increased until 4 s, which was again close to T_1, and then decreased after 4 s.

Table 7 T_1 of phospholipids and PSER in various sample matrices by ^{31}P NMR.

Sample	Mole ratio of cholic acid and total phospholipid including PSER	T_1 (s)							
		PC	SM	PI	PE	PS	PA	LPC	PSER
DOPC (High purity)	14:1	0.9	-	-	-	-	-	-	4.2
DOPS (High purity)	14:1	-	-	-	-	0.9	-	-	4.1
SM (High purity)	14:1	-	1.0	-	-	-	-	-	4.3
Soy lecithin 1	4.3:1	0.9	-	0.8	0.9	-	1.7	1.0	1.3
Soy lecithin 2	5.3:1	1.0	-	0.6	1.1	-	1.6	0.8	1.7
	6.9:1	1.0	-	0.7	1.0	-	-	1.1	1.8
	9.6:1	1.1	-	0.7	1.4	-	-	1.4	2.4
	16:1	1.1	-	1.0	-	-	-	-	3.2
PS dietary supplement food 1	24:1	-	-	-	-	0.9	-	-	2.1
PS dietary supplement food 2	9.8:1	-	-	-	-	0.8	-	-	3.1

All test solution concentrations determined using the ^{31}P NMR method.

The area intensity of an NMR spectrum generally increases with the recovery of

magnetization when the pulse interval time is extended, and eventually stabilizes with constant intensity. For quantitative NMR experiments using AQARI, to ensure that the signal area intensity for an observed nucleus correlated with the nuclear number, a pulse interval time more than five times longer than T_1 is required for stabilization[9]. However, in the present ^{31}P NMR of phospholipids in the surfactant solution, the area intensity decreased unexpectedly as the pulse interval time increased. Table 8 shows the quantitative values of DOPC at each pulse interval time. As mentioned in section 3.3.1, the purity of DOPC was determined to be 99.1% from the quantitative ^{1}H NMR result referencing the *N*-methyl group. Quantitative values of 98.8 and 99.0% were also obtained by ^{31}P NMR when the pulse interval time was 20 and 40 s, which were more than five times longer than the T_1 of DOPC (0.9 s) and PSER (4.2 s), respectively. An equivalent purity (98.7%) was also obtained at a pulse interval time of 2 s, which was half the T_1 of DOPC and PSER.

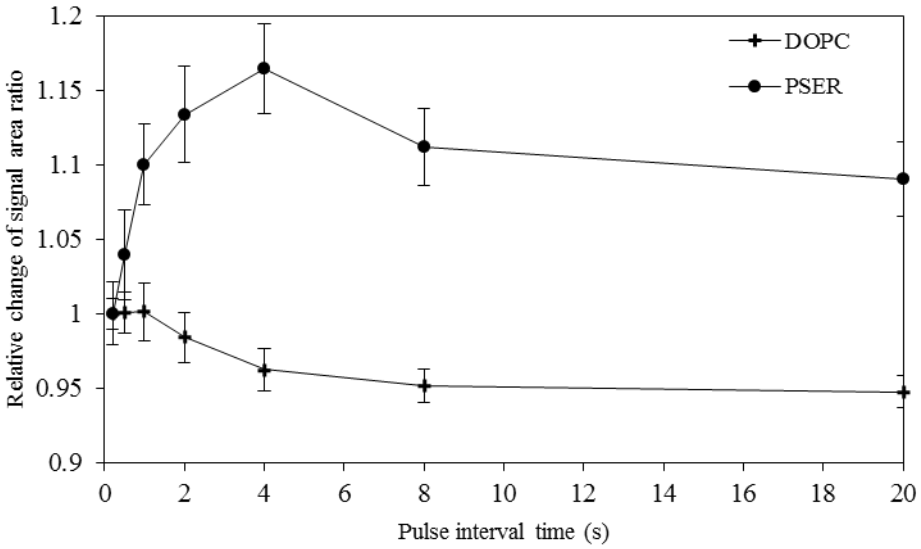

Fig. 14 Relative change in signal area ratio (DOPC and PSER) by ^{31}P NMR using various pulse interval times.

Area of initial point (0.2 s) set to 1, area at each pulse interval time expressed as a relative value. DOPC (9.96 mg/mL) in a surfactant solution with PSER (0.45 mg) as IS. Measurement conditions: probe temp, 30 °C; 2048 transients; spinning, on; ^{1}H decoupling, WALTZ.

Table 8 Phospholipid quantities using various relaxation delays.

Sample	Phospholipid	Relaxation delay (s)							Mean (%)	RSD (%)
		1	2	4	8	10	20	40		
DOPC	DOPC	103	98.7	94.0	97.3	-	98.8	99.0	98.5	3.0
Soy lecithin 1	PC	24.2	24.1	24.3	24.4	24.5	-	24.1	24.3	0.7
	PI	13.8	13.7	13.8	14	13.7	-	13.8	13.8	0.8
	PE	24.9	24.6	24.8	25	24.8	-	24.8	24.8	0.5
	PA	5.3	5.4	5.3	5.2	5.1	-	5.1	5.2	2.3
Dietary supplement 2	PS	20.5	19.5	18.7	18.7	18.9	-	19.4	19.3	3.6
	PA	2.6	2.5	2.4	2.3	2.3	-	2.4	2.4	4.8
	2-LPS	0.6	0.6	0.6	0.6	0.6	-	0.5	0.6	7.0

2-LPS: 2-lysophosphatidylserine

Test solutions of ^{31}P NMR were prepared for soy lecithin 1 and PS dietary supplement food 2. The phospholipid quantities were determined by changing the pulse interval time from 1 to 40 s over six steps. The obtained signal area of each phospholipid was compared with that of PSER, with the relationship between signal area and pulse interval time shown in Fig. 15. The phospholipid classes of soy lecithin 1 and PSER had T_1 values as low as 1 s, with the area intensity of these signals decreasing with increasing pulse interval time. The plots of all phospholipids and PSER showed a similar tendency of downward-sloping curves, and reasonable quantitative values with less than 1% RSD were obtained for PC, PI, and PE at all pulse interval times. Owing to the relatively low total phospholipid concentrations in PS dietary supplement food 2, the curves indicated that the area intensities of each compound had different tendencies at each pulse interval time, with the dispersion of quantitative values (4–7% RSD) becoming larger than that of soy lecithin 1 (>1% RSD). Quantitative values fluctuated up and down, even when the pulse interval time was extended to be close to T_1. In addition, as the similar case of the present study, the quantification of phospholipid classes by ^{31}P NMR using sodium cholate did not showed a significant difference in signal intensities between the case

where the pulse interval time is 1 s and that of 10 s. Moreover, acceptable signal intensity was also obtained from LPE of minor component at 3 s[55]. A relatively short interval time of 2 s was accordingly employed in the present study, not only for obtaining adequate quantification results, but also for reducing the time needed for data acquisition.

For accurate quantification of the samples containing unknown classes and concentrations of phospholipids, a suitably long pulse interval time compared with T_1 is desirable. However, such a strategy was not effective in the present case. In the surfactant solution, it was difficult to investigate the reason why the signal area of phospholipids and PSER decreased with the increasing the pulse interval time. As shown in the above results, for ^{31}P NMR quantification of 1–4 wt% phospholipid samples with a large molar ratio of surfactant, a short interval time of 2 s was effective for reducing the quantitative error to less than 5%. Therefore, the present method was confirmed as a reliable quantitative method.

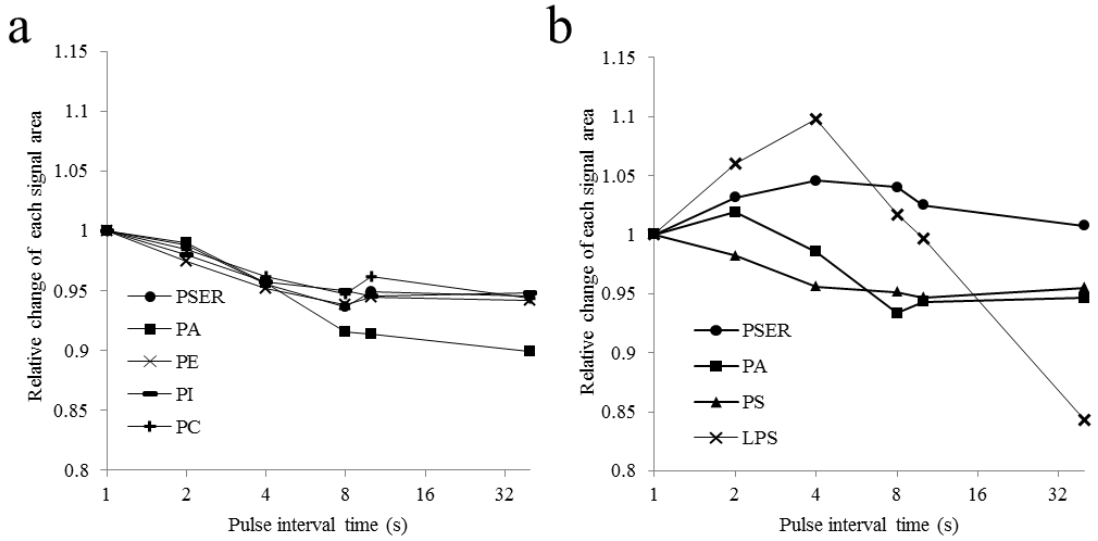

Fig. 15 Relative change in the signal area ratio (soy lecithin 1 and PS dietary supplement food 2) by ^{31}P NMR using various pulse interval times.

(a) Soy lecithin 1 (0.1 g) in surfactant solution (1.8 mL) with PSER (1.2 mg) as IS; probe temp, 30 °C; 2048 transients; spinning, on; ^{1}H decoupling, WALTZ.

(b) PS dietary supplement food 2 (0.1 g) in surfactant solution (1.8 mL) with PSER (0.98 mg) as IS; probe temp, 30 °C; 2048 transients; spinning, on; ^{1}H decoupling, WALTZ.

3.3.4 Effect of signal-to-noise ratio on quantitative area ratio by ^{31}P NMR

The test solution of soy lecithin 1 and PS dietary supplement food 2 was measured by ^{31}P NMR using a pulse interval time of 2 s while changing the number of integrations from 2 to 2048. As a result, the signal intensities of PS spectra were increased and the signal-to-noise ratios (S/N) were improved from 10 to 270. The signal area ratio of PS to PSER was calculated to be 103% from the spectrum with a S/N of 20, based on that from the spectrum with a S/N of 270 as 100%. However, the area ratio increased to 114% due to the influence of noise at S/N = 10. As soybean lecithin contained minor components, such as phosphatidylglycerol (PG) and 2-lysophosphatidic acid (2-LPA), more than 1024 scans were required to obtain an S/N of at least 20 using a 500-MHz NMR spectrometer.

3.3.5 Determination of phospholipids in polar lipids

^{31}P NMR spectra of polar lipid samples prepared from soy, brain, and yeast were measured and are shown in Fig. 16. The total phospholipid contents in the samples were 76.0 ± 0.3, 68.0 ± 0.3, and 82.6 ± 0.0%, respectively, determined by molybdenum blue colorimetry. As NMR enables determination of the molar amount in principal, the individual quantities of different phospholipid classes were directly calculated as molar amounts per 100 g of sample (Tables 9–11). The major phospholipid classes with contents of 10 mmol or more showed good repeatability, with RSDs of 0.5–2.1%. For phospholipid classes with contents of ≥1 mmol and <1 mmol, the repeatability varied significantly, with RSDs of 0.7–11% and 4.2–40%, respectively. Phospholipids and lysophospholipids are generally attached to one and two fatty acids, respectively, with carbon numbers of 16–20. Therefore, their molecular weights were calculated as species containing one and two stearic acid (C18) moieties as a typical fatty acid. Furthermore, the molybdenum blue colorimetric and 2D-TLC methods conventionally attributed the phospholipid content as stearoyloleoylphosphatidylcholine (SOPC)[51]. The results of ^{31}P NMR were also translated into SOPC quantities for comparison. The total phospholipid

contents of polar lipids prepared from soy, brain, and yeast obtained by ^{31}P NMR were in good agreement with those obtained by molybdenum blue colorimetry, in the range 97–102%. However, in comparison with the 2D-TLC method, the quantitative values provided by ^{31}P NMR were tended to higher (99–107%) because additional separation and extraction steps were not required for ^{31}P NMR. The main phospholipid class, with contents of 10% or more for all polar lipids, gave quantities by ^{31}P NMR up to 20% (97–117%) higher than those provided by the 2D-TLC method. Conversely, in phospholipid classes with contents of less than 10%, excluding PA, the ^{31}P NMR quantities remained low, at 13–79%. For the brain polar lipid, a low PA content (0.2%) was detected by ^{31}P NMR, but a quantitative value 10 times higher was obtained by 2D-TLC. Therefore, although differences between the results of ^{31}P NMR and 2D-TLC were relatively large for the individual quantification of phospholipid classes, ^{31}P NMR had the fundamental advantage of being less susceptible to handling errors during operation. Furthermore, ^{31}P NMR was able to quantify 1-lyso and 2-lyso forms, which are difficult to differentiate using the conventional method. Additionally, by converting results to an amount of SOPC, the ^{31}P NMR results were easily to compare with quantities obtained by the conventional method. These two methods would be cooperative in the case for the situation aimed for accuracy and contemporaneousness, such as availability of an NMR instrument and/or number of samples to be treated.

3.4. Conclusion

To accurately determine phospholipid classes in commercial foods and dietary supplements, the author optimized the ^{31}P NMR quantification method using a surfactant solution of cholic acid and verified its performance. Chemical shifts of phospholipids were highly reproducible when the test solution pH was adjusted to 6.90 ± 0.04. The pulse interval time and number of scans were optimized to obtain NMR signals suitable for quantitative calculation. The NMR signals of the phospholipids and PSER in surfactant micelles showed a

decreased signal area ratio at longer pulse interval times. The quantitative result equivalent to the quantity obtained by ^{1}H NMR, which is a reliable quantitative method, was obtained by ^{31}P NMR when the pulse interval time was more than 20 s, which was more than five times longer than the T_1 of phospholipids and PSER, respectively. However, the author found even at an interval time of 2 s, which was relatively short compared with T_1 can give the satisfactory results with the same degree of accuracy as the previous result. The optimized pulse interval time was successfully applied to quantify samples rich or moderately rich in phospholipids, such as lecithin, prepared from soybean, egg yolk, and PS dietary supplements. Using PSER as an internal standard TRM, the present method achieved SI traceability and confirmed its robustness in comparison with AQARI-based ^{1}H NMR using 1,4-BTMSB-d_4 CRM. Furthermore, ^{31}P NMR also accomplished concomitant analysis of many phospholipid classes, which is difficult to achieve using ^{1}H NMR. The optimized ^{31}P NMR method was successfully applied to the quantification of phospholipid classes in three types of polar lipid samples. The total phospholipid amount determined by ^{31}P NMR was in good agreement with total values obtained by conventional molybdenum blue colorimetry. In particular, the present method provided superior individual quantification of phospholipid classes compared with 2D-TLC, which required careful operation.

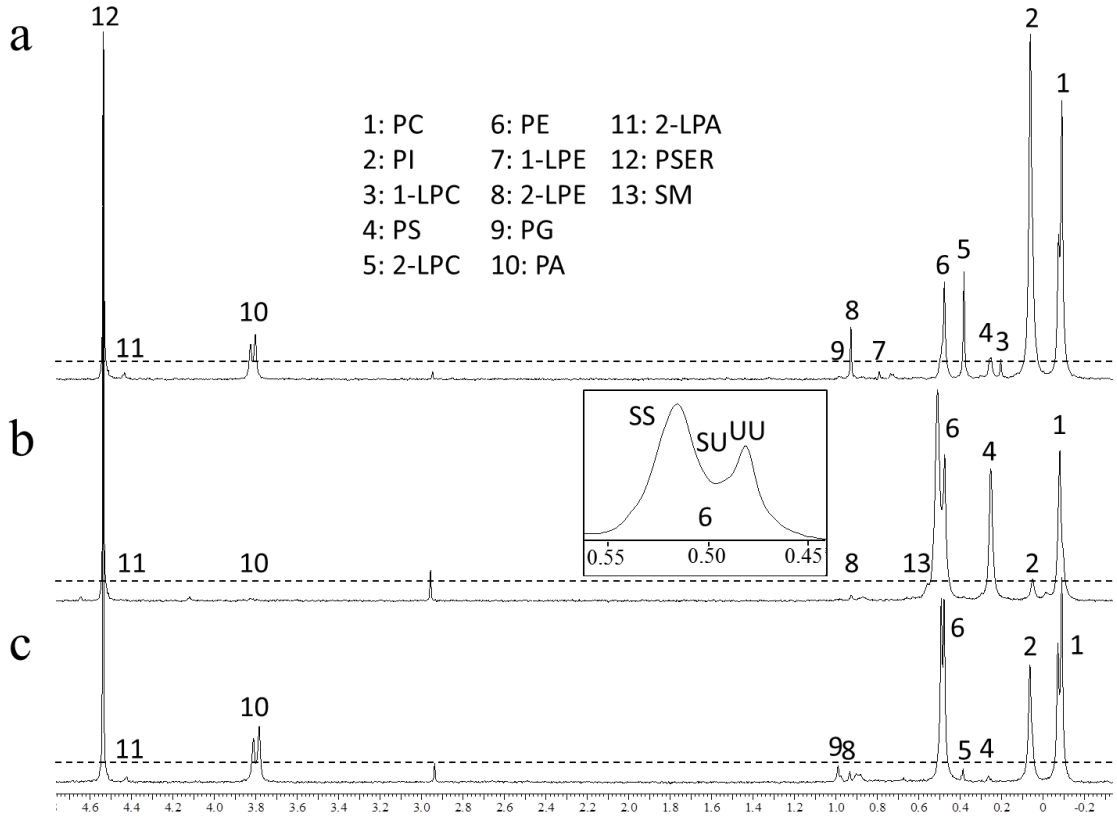

Fig. 16 ^{31}P NMR spectra of phospholipid classes in polar lipids (N = 3).

(a) Yeast polar lipid extract (30–38 mg), (b) brain (porcine) polar lipids extract (31–34 mg), and (c) soy polar lipid extract (25 mg) in of surfactant solution (2 mL) with PSER (0.5 mg) as IS; probe temp, 30 °C; 2048 transients; spinning, on; ^{1}H decoupling, WALTZ. A broken line represents the recommended quantification lower limit level, indicating a signal-to-noise ratio of 20. The PE with double saturated fatty acids is shown as SS, the PE with mixed saturated/unsaturated fatty acids is SU, and the PE with double unsaturated fatty acids is shown as UU. Each phospholipid signal was assigned using Table 6.

Table 9 Phospholipid class quantities in soy polar extract (100 g).

Method		^{31}P NMR			2D-TLC
Result		PL content (mmol)	DS form PL (wt%)	SOPC (wt%)	SOPC (wt%)
Class	PC	32.16 ± 0.27	25.4 ± 0.2	25.4 ± 0.2	25.3 ± 1.0
	PE	32.17 ± 0.21	24.1 ± 0.2	25.4 ± 0.2	21.8 ± 0.7
	PI	17.18 ± 0.09	14.9 ± 0.1	13.6 ± 0.1	14.0 ± 1.0
	PA	11.06 ± 0.14	7.8 ± 0.1	8.7 ± 0.1	4.3 ± 0.7
	PG	1.79 ± 0.05	1.4 ± 0.0	1.4 ± 0.0	3.8 ± 0.7
	PS	0.75 ± 0.07	0.6 ± 0.1	0.6 ± 0.1	-
	2-LPC	1.05 ± 0.09	0.6 ± 0.0	0.8 ± 0.1	3.1 ± 0.3
	2-LPE	0.83 ± 0.04	0.4 ± 0.0	0.7 ± 0.0	-
	2-LPA	0.48 ± 0.07	0.2 ± 0.0	0.4 ± 0.1	-
Total		97.47 ± 0.37	75.3 ± 0.3	76.9 ± 0.3	72.2 ± 1.7 (76.0 ± 0.3*)

DS from PL (^{31}P NMR): Absolute quantity calculated by multiplying the molar amount (mmol) by the molecular weight of distearoyl or lysostearoylphospholipid.

SOPC (^{31}P NMR): Absolute quantity calculated by multiplying the molar amount (mmol) by the molecular weight of SOPC.

*Quantitative value before separation by 2D-TLC.

Table 10 Phospholipid class quantities in brain (porcine) polar extract (100 g).

Method		^{31}P NMR			2D-TLC
Result		PL content (mmol)	DS form PL (wt%)	SOPC (wt%)	SOPC (wt%)
Class	PC	17.84 ± 0.35	14.1 ± 0.3	14.1 ± 0.3	13.9 ± 0.1
	PE	15.48 ± 0.15	32.4 ± 0.7	34.2 ± 0.7	29.5 ± 1.2
	PI	3.32 ± 0.03	2.9 ± 0.1	2.6 ± 0.0	3.6 ± 0.3
	PA	0.25 ± 0.05	0.2 ± 0.1	0.2 ± 0.0	2.9 ± 0.4
	PS	16.17 ± 0.16	12.8 ± 0.1	12.8 ± 0.1	11.2 ± 0.5
	2-LPE	0.33 ± 0.12	0.2 ± 0.1	0.3 ± 0.1	2.3 ± 0.5
	SM	1.99 ± 0.14	1.4 ± 0.1	1.6 ± 0.1	2.7 ± 0.3
	2-LPA	0.12 ± 0.05	0.1 ± 0.1	0.1 ± 0.0	-
Total		83.38 ± 1.04	64.0 ± 0.8	65.8 ± 0.8	66.2 ± 0.5 (68.0 ± 0.3*)

DS from PL (^{31}P NMR): Absolute quantity calculated by multiplying the molar amount (mmol) by the molecular weight of distearoyl or lysostearoylphospholipid.

SOPC (^{31}P NMR): Absolute quantity calculated by multiplying the molar amount (mmol) by the molecular weight of SOPC.

*Quantitative value before separation by 2D-TLC.

Table 11 Phospholipid class quantities in yeast polar extract (100 g).

Method		^{31}P NMR			2D-TLC
Result		PL content (mmol)	DS form PL (wt%)	SOPC (wt%)	SOPC (wt%)
Class	PC	32.81 ± 0.49	26.0 ± 0.4	25.9 ± 0.4	23.4 ± 1.0
	PE	9.76 ± 0.12	7.3 ± 0.1	7.7 ± 0.1	8.2 ± 0.4
	PI	43.09 ± 0.22	37.4 ± 0.2	34.0 ± 0.2	30.0 ± 1.2
	PA	7.10 ± 0.10	5.0 ± 0.1	5.6 ± 0.1	5.0 ± 0.6
	PG	0.35 ± 0.15	0.3 ± 0.1	0.3 ± 0.1	-
	PS	3.03 ± 0.06	2.4 ± 0.1	2.4 ± 0.1	-
	LPC	7.51 ± 0.07	3.9 ± 0.1	5.9 ± 0.1	7.5 ± 0.9
	2-LPC	6.37 ± 0.19	3.3 ± 0.1	5.0 ± 0.1	-
	1-LPC	1.14 ± 0.12	0.6 ± 0.1	0.9 ± 0.1	-
	LPE	2.84 ± 0.04	1.4 ± 0.1	2.2 ± 0.1	4.7 ± 0.2
	2-LPE	2.52 ± 0.06	1.2 ± 0.1	2.0 ± 0.1	-
	1-LPE	0.32 ± 0.03	0.2 ± 0.1	0.3 ± 0.1	-
	2-LPA	0.52 ± 0.05	0.2 ± 0.1	0.4 ± 0.1	-
Total		107.00 ± 0.55	83.8 ± 0.4	84.4 ± 0.4	78.8 ± 0.7 (82.6 ± 0.0*)

DS from PL (^{31}P NMR): Absolute quantity calculated by multiplying the molar amount (mmol) by the molecular weight of distearoyl or lysostearoyl-phospholipid.

SOPC (^{31}P NMR): Absolute quantity calculated by multiplying the molar amount (mmol) by the molecular weight of SOPC.

*Quantitative value before separation by 2D-TLC.

Discussion

1 Determination of polyether compounds quantity using AQARI

The author has used AQARI to quantify polymeric polyether compounds with molecular weights from 805 to 1,111. In the ^{1}H NMR of any of the compounds, signals derived from a large number of protons overlapped with each other in the high magnetic field region (0.5–2.5 ppm) derived from saturated hydrocarbons, making it difficult to use for quantification. Of the protons (3.5–5.0 ppm) bound to the oxycarbon and olefinic protons (5.0–6.5 ppm), relatively good separation signals were used for quantification. The skeleton of the polyether compound is flexible and takes various conformations. In this study, the ^{1}H NMR of the polyether compound showed a characteristic behavior, not seen with other organic compounds. In the spectrum of OA, the signal shape was broader with decreasing sample concentration. In particular, while H-14 and 15 protons belong to the same unsaturated double bond, the signal derived from the H-14 proton was always broader than H-15 and unsuitable for quantification. But H-15 proton was applicable to quantitative calculations up to a concentration of 0.01 mg/mL.

In CTXs, the all signals of protons residing on the cyclic structure of the main body were broadened in shape, and were difficult to apply to quantitative calculation. On the other hand, olefinic protons on the side chain were not broadened and the sharp signals were obtained. So these signals were used for the quantification of CTX1B, epideoxyCTX1B and CTX4A. However, CTX3C and 51hydroxyCTX3C, which do not have side chains, were forced to use the broadened signals. In the case of CTXs, it was judged that the quantifiable concentration by a general-purpose 500 MHz NMR instrument was 0.05 mg/mL. By using residual protons in the deuterated solvent as a removable IS, AQARI enable safely to use for quantification of highly precious substances. Because of the advantage of qNMR as a nondestructive analysis method, the sample can be recovered and used as a standard solution to another instrument analysis method such as chromatography. From the present results, the lower limit of quantitation of high

molecular weight organic compounds without repeating unit structure using NMR equipment with magnetic resonance frequency 500 MHz was 0.01–0.05 mg/mL with respect to molecular weight 800–1,000.

2 Determination of phospholipid quantity using AQARI based ^{31}P NMR

The individual phospholipid classes could be well separated by dispersing in aqueous cholic acid solution containing EDTA. The pH range of the sample solution and the measurement temperature were strictly controlled to be constant (pH 6.90 ± 0.04 at 30.0 ± 0.1 °C) in order to maintain the reproducibility of separation between phospholipid classes on the ^{31}P NMR spectrum. The author optimized the pulse interval time and the number of scans in order to improve the accuracy of AQARI based ^{31}P NMR. Thus, the deviation from the quantitative value by AQARI based ^{1}H NMR was successfully reduced within 5%. The good separation between phospholipid classes due to differences in hydrophilic groups bound to phosphate groups is unique characteristics to ^{31}P NMR. The phospholipid classes contained in foods such as soy lecithins and dietary supplements could be individually quantified by ^{31}P NMR. Compared with the existing 2D-TLC, ^{31}P NMR is simple in test operation and does not depend on the competence of analysts. Separation of individual phospholipid classes by ^{31}P NMR is also superior to 2D-TLC. Consequently, AQARI based ^{31}P NMR is a competitive-method in the quantification of phospholipids.

Acknowledgments

The author would like to thank Takeshi Yasumoto, a professor emeritus at Tohoku University and a member of the Japan Academy, for providing 60 mg of precious okadaic acid and five priceless CTXs for the present study. His passion for research gave me great courage to carry out this study.

The author would like to thank Naoki Sugimoto from National Institute of Health Sciences, Hiroaki Utsumi and Takako Suematsu from JEOL RESONANCE Inc. for their help to measure highly sensitive NMR spectra of CTXs.

The author is grateful to Maki Saito and Kana Yamamoto for active support of processing for ^{1}H NMR spectra.

The author wishes to thank Mami Nishimiya, Kyoko Kishida, Akiko Kawata and Kounosuke Suzuri for development of ^{31}P NMR method in phospholipid analysis.

The author would like to thank Mika Nagae, Kazuhiro Fujita, Munetomo Nakamura, Tomoji Igarashi and Masatoshi Watai for useful advices and encouraging words.

The author would like to thank to all co-workers of section of Applied Testing (Japan Food Research Laboratories) for kind considerations.

Finally, the author wishes to thank Prof. Minoru Inagaki from bottom of my heart for his careful guidance throughout this study.

References

[1] Saito, T., Ihara, T., Sato, H., Jancke, H., Kinugasa, S. 2003. International comparison on the determination of an ethanol aqueous solution by ^{1}H nuclear magnetic resonance. *Bunseki Kagaku*, **52**, 1029–1036.

[2] Wang, H., Ma, K., Zhang, W., Li, J., Sun, G., Li, H. 2012. Certification of the reference material of water content in water saturated 1-octanol by Karl Fischer coulometry, Karl Fischer volumetry and quantitative nuclear magnetic resonance. *Food Chem*. **134**, 2362–2366.

[3] Li, Z. Y., Welbeck, E., Wang, R. F., Liu, Q., Yang, Y. B., Chou, G. X., Bi, K. S., Wang, Z. T. 2015. A universal quantitative ^{1}H nuclear magnetic resonance (qNMR) method for assessing the purity of dammarane-type ginsenosides. *Phytochem. Anal*. **26**, 8–14.

[4] Wider, G., Dreier, L. 2006. Measuring protein concentrations by NMR spectroscopy. *J. Am. Chem. Soc*. **128**, 2571–2576.

[5] Barantin, L., Le Pape, A., Akoka, S. 1997. A new method for absolute quantitation of MRS metabolites. *Magn. Reson. Med*. **38**, 179–182.

[6] Farrant, R. D., Hollerton, J. C., Lynn, S. M., Provera, S., Sidebottom, P. J., Upton, R. J. 2010. NMR quantification using an artificial signal. *Magn. Reson. Chem*. **48**, 753–762.

[7] Cullen, C. H., Ray, G. J., Szabo, C. M. 2013. A comparison of quantitative nuclear magnetic resonance methods: internal, external, and electronic referencing. *Magn. Reson. Chem.* **51**, 705–713.

[8] Miura, T., Sugimoto, N., Suematsu, T., Millis, K.K., Asakura, K., Yamada, Y. 2017. Analytical standards purity determination using quantitative nuclear magnetic resonance. In Tomioka, K., Shioiri, T., Sajiki, H., Eds., *New Horizons of Process Chemistry: Scalable Reactions and Technologies* (275–285). Singapore: Springer.

[9] Saito, T., Nakaie, S., Kinoshita, M., Ihara, T., Kinugasa, S., Nomura, A., Maeda, T. 2004. Practical guide for accurate quantitative solution state NMR analysis. *Metrologia*. **41**, 213–218.

[10] Hosoe, J., Sugimoto, N., Suematsu, T., Yamada, Y., Miura, T., Hayakawa, M., Suzuki, H., Katsuhara, T., Nishimura, H., Kikuchi, Y., Yamashita, T., Goda, Y. 2014. Preliminary studies for application of quantitative NMR (qNMR) in the Japanese pharmacopoeia (1). *Pharm. Med. Device Regul. Sci.* **45**, 243–250.

[11] Ohtsuki, T., Sato, K., Sugimoto, N., Akiyama, H., Kawamura, Y. 2012. Absolute quantitative analysis for sorbic acid in processed foods using proton nuclear magnetic resonance spectroscopy. *Anal. Chim. Acta*. **734**, 54–61.

[12] Ohtsuki, T., Sato, K., Sugimoto, N., Akiyama, H., Kawamura, Y. 2012. Absolute quantification for benzoic acid in processed foods using quantitative proton nuclear magnetic resonance spectroscopy. *Talanta*. **99**, 342–348.

[13] Saito, T., Ihara, T., Koike, M., Kinugasa, S., Fujimine, Y., Nose, K., Hirai, T. 2009. A new traceability scheme for the development of international system-traceable persistent organic pollutant reference materials by quantitative nuclear magnetic resonance. *Accred. Qual. Assur*. **14**, 79–86.

[14] Weber, M., Hellriegel, C., Rück, A., Sauermoser, R., Wüthrich, J. 2013. Using high-performance quantitative NMR (HP-qNMR®) for certifying traceable and highly accurate purity values of organic reference materials with uncertainties <0.1%. *Accred. Qual. Assur*. **18**, 91–98.

[15] Yamazaki, T., Eyama, S., Takatsu, A. 2017. Concentration measurement of amino acid in aqueous solution by quantitative ^{1}H NMR spectroscopy with internal standard method. *Anal. Sci*. **33**, 369–373.

[16] Yasumoto, T., Oshima, Y., Yamaguchi, M. 1978. Occurrence of a new type of shellfish poisoning in the Tohoku district. *Bull. Japan. Soc. Sci. Fish*. **44**, 1249–1255.

[17] Tachibana, K., Scheuer, P. J., Tsukitani, Y., Kikuchi, H., Engen, D. V., Clardy, J., Gopichand, Y., Schmitz, F. J. 1981. Okadaic acid, a cytotoxic polyether from two marine sponges of the genus Halichondria. *J. Am. Chem. Soc*. **103**, 2469–2471.

[18] Yasumoto, T., Oshima, Y., Sugawara, W., Fukuyo, Y., Oguri, H., Igarashi, T., Fujita, N. 1980. Identification of dinophysis fortii as the causative organism of diarrhetic shellfish poisoning. *Bull. Japan. Soc. Sci. Fish*. **46**, 1405–1411.

[19] Murakami, Y., Oshima, Y., Yasumoto, T. 1982. Identification of okadaic acid as a toxic component of a marine dinoflagellate prorocentrum lima. *Bull. Japan. Soc. Sci. Fish*. **48**, 69–72.

[20] Alexander, J., Auðunsson, G. A., Benford, D., Cockburn, A., Cravedi, J., Dogliotti, E., Domenico, A. D., Fernández-Cruz, M. L., Fink-Gremmels, J., Fürst, P., Galli, C., Grandjean, P., Gzyl, J., Heinemeyer, G., Johansson, N., Mutti, A., Schlatter, J., Leeuwen, R. V., Peteghem, C. V., Verger, P. 2008. Marine biotoxins in shellfish–okadaic acid and analogues scientific opinion of the panel on contaminants in the food chain. *EFSA J.* **589**, 1–62.

[21] Suzuki, T., Quilliam, M. A. 2011. LC-MS/MS analysis of diarrhetic shellfish poisoning (DSP) toxins, okadaic acid and dinophysistoxin analogues, and other lipophilic toxins. *Anal. Sci*. **27**, 571–584.

[22] Stabell, O. B., Hormazabal, V., Steffenak, I., Pedersen, K. 1991. Diarrhetic shellfish toxins: improvement of sample clean-up for HPLC determination. *Toxicon*, **29**, 21–29.

[23] Draisci, R., Croci, L., Giannetti, L., Cozzi, L., Lucentini, L., De Medici, D., Stacchini, A. 1994. Comparison of mouse bioassay, HPLC and enzyme immunoassay methods for determining diarrhetic shellfish poisoning toxins in mussels. *Toxicon.* **32**, 1379–1384.

[24] Quilliam, M. A. 1995. Analysis of diarrhetic shellfish poisoning toxins in shellfish tissue by liquid chromatography with fluorometric and mass spectrometric detection. *J. AOAC Int.* **78**, 555–570.

[25] Burton, I. W., Quilliam, M. A., Walter, J. A. 2005. Quantitative ^{1}H NMR with external standards: use in preparation of calibration solutions for algal toxins and other natural products. *Anal. Chem*. **77**, 3123–3131.

[26] Perez, R., Rehmann, N., Crain, S., LeBlanc, P., Craft, C., MacKinnon, S., Reeves, K., Burton, I. W., Walter, J. A., Hess, P., Quilliam, M. A., Melanson, J. E. 2010. The preparation of certified calibration solutions for azaspiracid-1, -2, and -3, potent marine biotoxins found in shellfish. *Anal. Bioanal. Chem*. **398**, 2243–2252.

[27] Watanabe, R., Suzuki, T., Oshima, Y. 2010. Development of quantitative NMR method with internal standard for the standard solutions of paralytic shellfish toxins and characterisation of gonyautoxin-5 and gonyautoxin-6. *Toxicon.* **56**, 589–595.

[28] Dominguez, H. J., Crespin, G. D., Santiago-Benitez, A. J., Gavin, J. A., Norte, M., Fernandez, J. J., Daranas, A. H. 2014. Stereochemistry of complex marine natural products by quantum mechanical calculations of NMR chemical shifts: solvent and conformational effects on okadaic acid. *Mar. Drugs*. **12**, 176–192.

[29] Yamazaki, T., Saito, T., Miura, T., Ihara, T. 2012. Investigation of analysis conditions for accurate quantitative NMR analysis. *Bunseki Kagaku*. **61**, 963–967.

[30] Sasaki, K., Onodera, H., Yasumoto, T. 1998. Applicability of the phenylglycine methyl ester to the establishment of the absolute configuration of dinophysistoxin-1, a polyether toxin responsible for diarrhetic shellfish poisoning *Enantiomer.* **3**, 59–63.

[31] Yasumoto, T. 2001. The chemistry and biological function of natural marine toxins. *Chem. Rec*. **1**, 228–242.

[32] Yasumoto, T. 2005. Chemistry, etiology, and food chain dynamics of marine toxins. *Proc. Jpn. Acad. Ser. B*. **81**, 43–51.

[33] Yasumoto, T., Inoue, A. Bagnis, R., Garcon, M. 1979. Ecological survey on a dinoflagellate possibly responsible for the induction of ciguatera. *Bull. Jpn. Soc. Sci. Fish.* **45**, 395–399.

[34] Yogi, K., Oshiro, N., Inafuku, Y., Hirama, M., Yasumoto, T. 2011. Detailed LC-MS/MS analysis of ciguatoxins revealing distinct regional and species characteristics in fish and causative alga from the Pacific. *Anal. Chem*. **83**, 8886–8891.

[35] Ikehara, T., Kuniyoshi, K., Oshiro, N., Yasumoto, T. 2017. Biooxidation of ciguatoxins leads to species-specific toxin profiles. *Toxins* **9**, doi:10.3390/toxins9070205.

[36] U.S. Food and Drug Administration. Fish and fishery products hazards and controls guidance, 4th ed. available online: https://www:fda.gov/food/guidanceregulation/guidancedocumentsregulatory information/seafood/ucm2018426.htm (accessed on 22 February 2019).

[37] Murata, M., Legrand, A.M., Ishibashi, Y., Fukui, M., Yasumoto, T. 1990. Structures and configurations of ciguatoxin from the moray eel Gymnothorax javanicus and its likely precursor from the dinoflagellate Gambierdiscus toxicus. *J. Am. Chem. Soc*. **112**, 4380–4386.

[38] Satake, M., Murata, M., Yasumoto, T. 1993. The structure of CTX3C, a ciguatoxin congener isolated from cultured Gambierdiscus toxicus. *Tetrahedron Lett*. **34**, 1975–1978.

[39] 2009. Phospholipids in lecithin concentrates by TLC. In American Oil Chemists' Soc., Ed., recommended practice (Ja 7–86).

[40] 1996. Phospholipid (thin layer chromatography method). In Japan Oil Chem. Soc., Ed., standard methods for the analysis of fats, oils and related materials (4.3.3.1–1996).

[41] 2007. Determination of lecithin phospholipids by HPLC-LSD. In American Oil Chemists' Soc., Ed., official method (Ja 7c–07).

[42] Pimentel, L., Gomes, A., Pintado, M., Rodríguez-Alcalá, M.L. 2016. Isolation and analysis of phospholipids in dairy foods. *J. Anal. Methods Chem*. **2016**, 1–12.

[43] Contarini, G., Povolo, M. 2013. Phospholipids in milk fat: composition, biological and technological significance, and analytical strategies. *Int. J. Mol. Sci.* **14**, 2808–2831.

[44] Vervoort N., Daemen, D., Török G. 2008. Performance evaluation of evaporative light scattering detection and charged aerosol detection in reversed phase liquid chromatography. *J Chromatogr. A* **1189**, 92–100.

[45] Spyros, A., Dais, P. 2009. ^{31}P NMR spectroscopy in food analysis. *Prog. Nucl. Mag. Res. Sp.* **54**, 195–207.

[46] Mets, K.R., Dunphy, L.K. 1996. Absolute quantitation of tissue phospholipids using ^{31}P NMR spectroscopy. *J. Lipid Res.* **37**, 2251–2265.

[47] Yao, L., Jung, S. 2010. ^{31}P NMR phospholipid profiling of soybean emulsion recovered from aqueous extraction. *J. Agric. Food Chem*. **58**, 4866–4872.

[48] London, E., Feigenson, G.W. 1979. Phosphorus NMR analysis of phospholipids in detergents. *J. Lipid. Res.* **20**, 408–412.

[49] Schiller, J., Arnold K. 2002. Applications of high resolution ^{31}P NMR spectroscopy to the characterization of the phospholipid composition of tissues and body fluids – a methodological review. *Med. Sci. Monit*. **8**, 205–222.

[50] MacKenzie, A., Vyssotski, M., Nekrasov, E. 2009. Quantitative analysis of dairy phospholipids by ^{31}P NMR. *J. Am. Oil. Chem. Soc.* **86**, 757–763.

[51] 2013. Phospholipid (Phospholipids). In Japan Oil Chem. Soc., Ed., standard methods for the analysis of fats, oils and related materials (2.4.11–2013).

[52] Diehl, B.W.K. 2001. High resolution NMR spectroscopy. *Eur. J. Lipid Sci. Technol*. **103**, 830–834.

[53] Dennis, E.A.; Plückthum, A. 1984. Phosphorus-31 NMR of phospholipids in micelles. in Gorenstein, D.G., Ed., *Phosphorus-31 NMR: principles and applications*. (pp. 423–446). New York, USA: Academic Press.

[54] Le Maire, M., Champeil, P., Moller, J.V. 2000. Interaction of membrane proteins and lipids with solubilizing detergents. *Biochim. Biophys. Acta* **1508**, 86–111.

[55] Lanier, K.L., Moore, J.D., Smith, D., Li, S., Davis, B., Shaw, W.A. 2008. Quantitative phospholipid analysis of soy lecithin and krill lecithin by ^{31}P NMR. available online: https://avantilipids.com/images/Analytical/AvantiPhospholipidAnalysis-AnalyticalServices.pdf (accessed on 22 February 2019).

List of Publications

The contents of this thesis have been published in the following original papers.

Chapter 1

Absolute Quantification of Lipophilic Shellfish Toxins by Quantitative Nuclear Magnetic Resonance Using Removable Internal Reference Substance with SI Traceability.

Tsuyoshi Kato, Maki Saito, Mika Nagae, Kazuhiro Fujita, Masatoshi Watai, Tomoji Igarashi, Takeshi Yasumoto, Minoru Inagaki

Analytical Sciences, 2016, **32 (7)**, 729-734

Chapter 2

Quantification of Representative Ciguatoxins in the Pacific Using Quantitative Nuclear Magnetic Resonance Spectroscopy.

Tsuyoshi Kato, Takeshi Yasumoto

Marine Drugs, 2017, **15 (10)**. pii:E309. doi: 10.3390/md15100309

Chapter 3

Quantitative ^{31}P NMR Method for Individual and Concomitant Determination of Phospholipid Classes in Polar Lipid Samples

Tsuyoshi Kato, Mami Nishimiya, Akiko Kawata, Kyoko Kishida, Kounosuke Suzuri, Maki Saito, Kazuhiro Fujita, Tomoji Igarashi, and Minoru Inagaki

Journal of Oleo Science, 2018, **67 (10)**, 1279-1289